The International Journal of Engineering and Science (IJES)
|| Volume || 13 || Issue || 8 || Pages || PP 109-151 || 2024 ||
ISSN (e): 2319 – 1813 ISSN (p): 2319 – 1805

Empowering Wearable Devices: Harnessing Ambient Energy for Sustainable Operation in IoT Systems

Pyae Han Kyaw[1]
[1]*The University of Newcastle, Australia*
Corresponding Author: PyaeHanKyaw@uon.edu.au

ABSTRACT
As wearable devices becomes more popular in recent years, these wearable devices drew attention as they can improve the quality of life. Some of these devices provide help to the healthcare professionals, especially for the patients who want to live independently without going to authorized places such as hospitals. They can monitor the patient's vital signs remotely. However, one of the major problems is that these devices need continuous power supply. These devices solely depend on the battery and when it is depleted, the operation of the device is affected. Hence to solve this problem, the efficient energy harvesting technology become crucial. So, this project is about harvesting the energy from different sources in which we can obtain from human and from the environment then capitalized to power to different applications such as wearable devices and portable energy harvesting devices. The energy harvesting systems gain significant attention as a promising solution for powering small scale electronic devices in many applications. This project explores the challenge and opportunities associated with harvesting energy from ambient sources and applies to one of the most well-known technologies known as Internet of things or IoT. The low voltage harvesting systems includes photovoltaic cells, Thermoelectric generators, piezoelectric material, and magnetic inductions. Furthermore, the harvested energy will be stored in a battery and will power the IoT system.

KEYWORDS;- *IoT applications, Energy harvesting, battery monitoring system, wearable and portable applications,*

Date of Submission: 24-08-2024 Date of acceptance: 03-09-2024

I. INTRODUCTION

As the aging populations has grown over time in worldwide, the improvement in quality of life is becoming more necessary. Many researchers predict that it will further increase in the aging populations because of that reason, the health care systems are facing the massive increase in cost and crowded in medical institutions. If we can reduce the medical systems small enough to carry around like wearable devices, we can solve these problems. Here are some of the problems that we can solve by wearing these wearable devices [1-6]:

A) Detections of medical illness
B) Emergency notifications
C) Computer assisted rehabilitation.
D) Health sectors for assisting the physical and mental health of the soldiers in combat etc. [7]

There are some energy limitations since most of the wearable devices are powered by the battery. When the battery is depleted or discharged completely, it must be replaced or recharge. This problem remains critical constraint. During the battery changing process the health monitoring system can be interrupted [11]. Hence the constant power supply become more compulsory. This project aims to solve this kind of power restriction problems and aims to extract the energy from every possible source as wearable device.

II. OBJECTIVE

This project aims to build prototypes of energy scavenging devices. In other words, this project goal is to develop a multiple energy scavenging system reflecting for wearable and portable applications. Then, manage them to charge up battery which we can later use for many applications such as remote corrosion monitoring systems, Structural monitoring, RFID, Implantable devices and remote patient monitoring, Internet of things and equipment monitoring.

The project must fulfill the following objectives:

- Research about various types of energy harvesting systems.

- Design the energy harvesting systems such as solar, thermal, wind, motion and mechanical stress for wearable and portable options.
- Simulate and develop a prototype for the sources and charges the Battery which are the sources for many usable options.
- Develop the IoT platform for monitoring battery as a application of energy harvesting.

III. LITERATURE REVIEW

Principle of operations of harvesting sources

Solar source

Solar cells are made of semiconductors. Specifically, they have three layers which are the combination of P-type and N-Type Semiconductors. The top layer thin and is made of silicon containing tiny amount of element such as phosphorus which have more electrons than the silicon. This give the top layer an excess of electrons that are free to move and make the material more conductive. Thus, the top layer is N-Type. The thin bottom layer is also made with silicon containing tiny amount of boron or gallium which have fewer electrons than silicon. This give the bottom layer fewer electrons that are free to move which make the bottom layer less conductive for electrons. Thus, the bottom layer is called P-Type. The middle layer is thicker than the top and bottom layer and only slightly fewer electrons making the material marginally P-type [8-17]. Thin metal lines usually made of silver are printed on the top of the top layer and the aluminum plate is contact with the bottom layer. The schematic representation of the solar cell can be found in the following Figure (2). We all know that sunlight have different wavelength and emit different waves. Some waves are visible to us, and some did not since the wavelength is too long to see such as inferred red light and some wavelength is too short to see such as ultraviolet. For solar cells only light with wavelength 350-1140nm are absorbed by it. These also include the visible lights. When the sunlight hit to the cell, the middle layer absorbs it and the light wave split the electron from the silicon atom which make the electron to lose and leaving the area of positive charge also called 'hole'. The loose electron moves to the top N-type layer and the 'hole' which are positively charge atom move toward the bottom P-type layer. Such effect is known as 'Photovoltaic Effect' and if the sunlight hit on the cell the process continues. Now that the electrons and the 'holes' are separated to each layer and when the wire is connected to the top and the bottom layer which make the electron to flow making the current [33-36]. In this project, the solar panels can be chosen as one of the energy sources since the sunlight can reach most of the places on earth especially in Asia regions. Making it to miniature size and make it like a wearable device is possible.

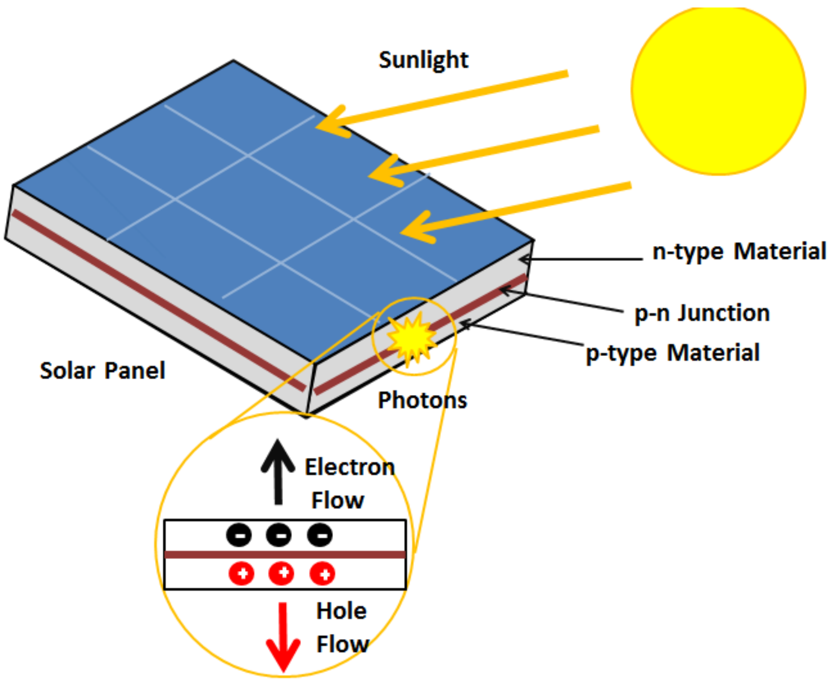

Figure 1: *Solar cell schematic and Photovoltaic effect*

Various Size and Types Solar Panels

There are so many varieties to choose as the size for solar panels, also choosing the right material for this project is also vitally important. Here are some of the materials that used in solar panels and their comparisons [36].

Table 1: Comparisons for all the solar panel materials and their specification comparisons

Material	Efficiency	Voltage	Current	Advantages	Disadvantages
Monocrystalline Silicon	20-22%	32-36V	6-10A	High efficiency, long lifespan, High temperature tolerance	Expensive to produce, Susceptible to shading
Polycrystalline Silicon	15-17%	28-32V	6-10A	Lower cost than mono-crystalline, good efficiency	Less efficient than mono-crystalline, Susceptible to shading
Thin-Film (CdTe)Cadmium Telluride	11-13%	60-80V	2-3A	Low production cost, Performs well in high temperature	Lower efficiency than silicon, shorter lifespan
Thin-Film Copper Indium Gallium Selenide (CIGS)	12-14%	30-40V	2-3A	Flexible, Performs well in low light conditions	Lower efficiency than silicon, shorter lifespan
Perovskite	20-25%	18-22V	10-12A	Low production cost, Easy to manufacture, High efficiency	Short lifespan, Poor stability in humid environments
Organic	5-8%	4-5V	1-2A	Low production cost, Flexible, Lightweight	Very low efficiency, short lifespan

There are several things to consider when it comes to wearable solar energy harvesting devices, such as flexibility, weight, robustness, and efficiency. Due to their flexibility and light weight, thin-film materials like Copper Indium Gallium Selenide (CIGS) and new technologies like Perovskite and Organic solar cells are particularly ideally suited for wearables [20-25]. Given their ability to be printed on flexible substrates and their small weight, organic solar cells have been found to be the most promising among them for wearable applications. They are also less expensive to create than other technologies. However, they may not be appropriate for applications requiring significant power production since their efficiency is currently lower than that of other types of solar cells,

[26] Overall, the ideal material for a wearable solar energy harvesting device will be determined by the application's specific requirements and limits, and it is critical to examine the trade-offs between flexibility, weight, durability, and efficiency while selecting a material. According to the above table the most suitable material for this project is Cadmium Telluride and Copper Indium Gallium Selenide which are mentioned above. Because of their flexibility and thin film property they are most suitable materials for this project. However, the materials are hard to get in the market, not very efficient and have shorter life span than that of other materials. Hence, this project will use Mono-crystalline Silicon material.

Thermal Energy Source

The thermal electric generators or TEG are the modules that convert heat source into an electrical energy with the temperature difference of the other side of the module itself. This effect is called 'Seek beck Effect' [34]. As we study furthermore about these modules, One Peltier Module consists of many semiconductors connected as thermal couple. One thermal coupled semiconductor can be seen in the below figure.

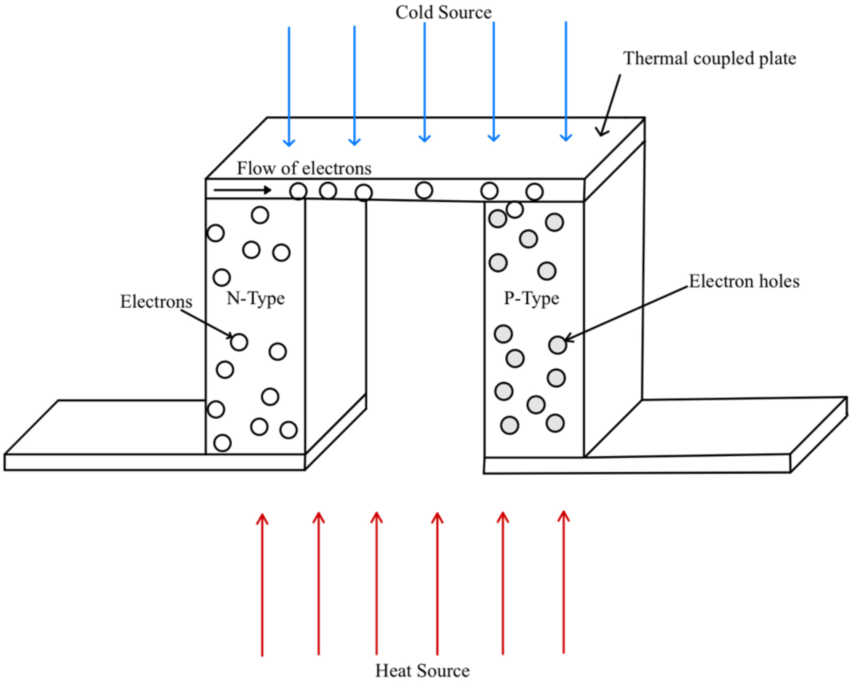

Figure 2: Two Semiconductors Thermal coupled & Seek Beck Effect

As the heat is applied to one end of the pair of semiconductors, the electron within them become excited, gain energy, and move toward the cooler end [14-19]. Since N-type have the excess of electrons and P-Type have the space to accept them, the electrons flow from the N-type to P-type semiconductor hence making the current. However, as for the voltage scale, it does not depend on the temperature but the difference between the heat and cold source. The larger the differential the larger the voltage will be. In order to use these modules as an energy harnessing system for this project, first we need the heat source. A healthy human can produce around 97°F(36.1°C) to 99°F(37.2°C) heat [15]. When we design with the proper heat sink for the cold surface, we can get a few millivolts and if we can use it with voltage booster circuit, we can also add this module as one of the energies harvesting system. The temperature difference to the voltage and current output of the SP1848-27145 can be observed in the flowing table.

Table 2: Temperature difference to the Voltage and current output of SP1848-27145 TEG

No.	Temperature Difference(°C)	Voltage (V)	Current(mA)
1	20	0.97	225
2	40	1.8	368
3	60	2.4	469
4	80	3.6	558
5	100	4.8	669

This module can withstand up to 150°C. There are already some commercial products existed like ‘miniO’ the miniature thermal electric generators.

Figure 3: SP1848-27145 TEG module

Bismuth telluride (Bi2Te3) is generally used material for small-scale wearable thermoelectric devices meant to harvest energy from human body heat due to its high efficiency at ambient temperature and good performance with low temperature differences. It also has a low melting point, making it appropriate for small-scale electronics [14].
Other materials, such as silicon germanium (SiGe) and magnesium silicide (Mg2Si), may be appropriate based on the device's unique needs and operating temperature range. However, when compared to bismuth telluride, these compounds are often less efficient at ambient temperature.

A thermoelectric generator's efficiency is determined by various parameters, including the temperature difference across the material, the size and shape of the material, and the overall design of the device [15]. As a result, it is critical to thoroughly analyze the wearable device's individual requirements and select the proper material accordingly. The comparison table for the TEG materials are as follow.

Table 3:Comparisons of TEG Materials

Material	Seebeck Coefficient	Efficiency	Pros	Cons
Bismuth Telluride	200-250 µV/K	5-8%	High efficiency at room temperature, good for low temperature differentials, low toxicity	Limited by high temperatures, low mechanical strength
Lead Telluride	250-300 µV/K	5-8%	High efficiency at high temperatures, good for high temperature differentials, low toxicity	Limited by low temperatures, low mechanical strength
Silicon Germanium	150-200 µV/K	6-10%	High efficiency over a wide temperature range, high mechanical strength	Expensive material, low output power
Sodium Cobaltite	300-400 µV/K	8-12%	High efficiency at high temperatures, good for high temperature differentials, high mechanical strength	Expensive material, limited by low temperatures
Magnesium Silicide	500-800 µV/K	5-8%	High efficiency at high temperatures, good for high temperature differentials, high mechanical strength	Limited by low temperatures, low durability

The best material for this project is Bismuth Telluride or ceramic because this is the only material that have the high efficiency under the room temperature since we must consider extracting the energy just from the human body heat [13]. Therefore, we will be using SP1848-27145 TEG module.

Wind Source

When seeking for the wind source from human body there is only a few factors. Even though the wing energy harvesting for industrial applications is viral nowadays there is only few options for wearable applications. We can gain wind energy when the human is walking or running by swinging their hands. However, it depends on many factors such as the design of the fan blade, the angular velocity of the arm to rotate the generator itself, the speed of an arm and many aerodynamic factors to gain maximum power while running or walking [27-32]. In addition, it is hard to simulate such factors and thus, in this project, the two motors will couple while one motor act like a motor to generate the approximate speed of the human hand swing and another motor will act like a generator to scavenge energy. Hence, choosing the viable motor for this project is necessity. There are so many variations of motors such as AC motors, DC motors, DC brushless motors, DC brush motors, stepper motors, servo motors etc. [6-16] As for this project the core-less DC motors are chosen because of the following reasons.

a. **High efficiency with compact design:** Compared to other motors in the market, these motors are usually lighter and have less current loss making them efficient than the cored types.
b. **Low drawing current:** Since it does not draw much current and in some case when want to reuse as a motor it will make the battery longer.
c. **Does not need much inertia:** The system only depends on the wind generated by hand swing hence the less inertia the better to harness energy.
d. **Last longer:** Without iron core only less chance to arcing and sparking which may lead the motor to last longer than the other motors if we do not have electromagnetic interference.
e. **Low noise:** These motors run very quietly when considering about as the wearable devices.

Core-less motors are usually brushless or brushed motors with a coil wound on to itself not on an iron [4-8]. They are wound in a special pattern like oblique or honeycomb design to create dense and self-supporting weave. Epoxy resin is then used to secure the weave in place. In brush motors, rare earth magnets make up the stator, which is situated in the interior of the motor. In brushless motors, the magnet, which is always internal, and it is part of the rotor.

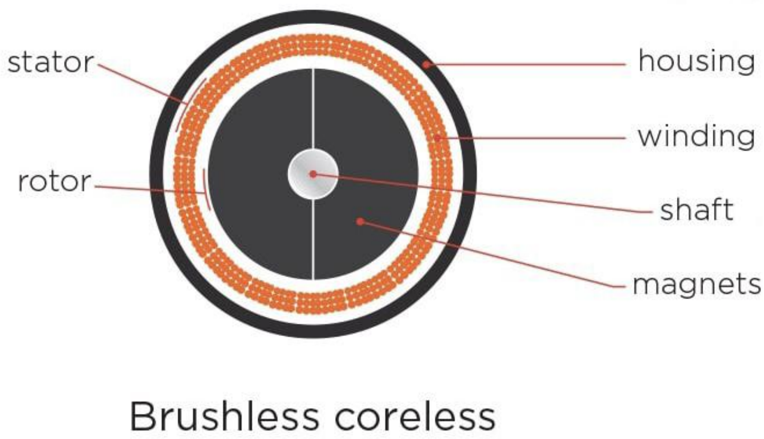

Figure 4: Cross sectional diagram of Brush Less Motor [6]

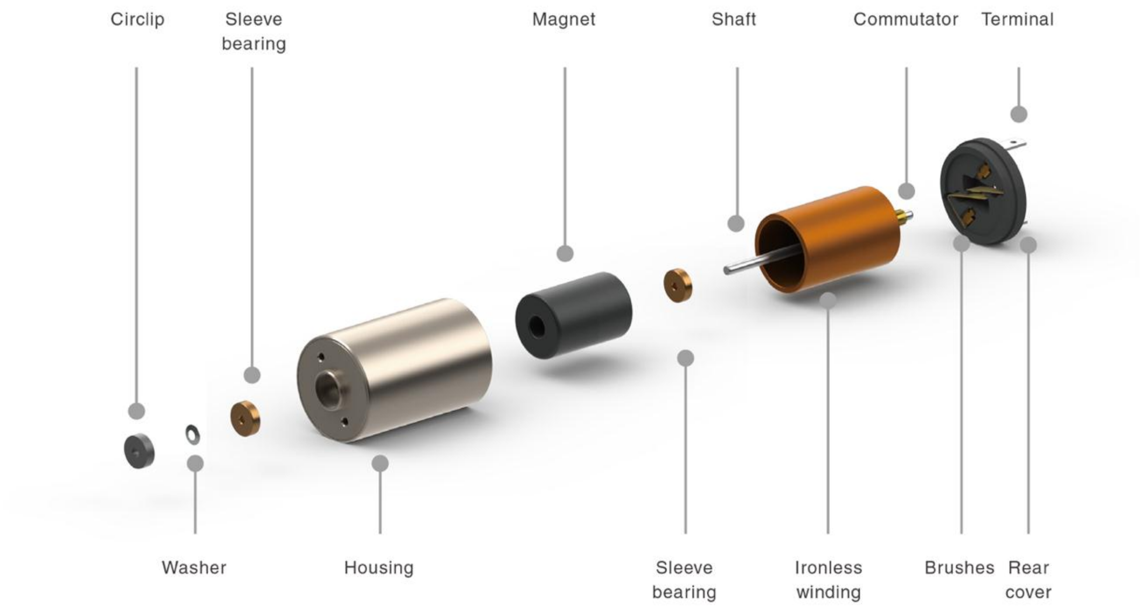

Figure 5: Inner Parts of the coreless DC motor [4]

Efficiency, dependability, and cost-effectiveness are the most crucial factors to consider while generating power by coupling motors together. In general, DC motors, stepper motors, and AC induction motors are some of the motor types that are frequently utilized to produce power. [4] The factor that the DC motors make an excellent choice for energy scavenging applications is that they are very easy to control and simple to use. They are constrained in some circumstances since they need a DC power supply to function.
Another choice is a stepper motor, which may produce power by manually turning the motor shaft but to transform the output into usable electrical power, stepper motors may need additional electronics, making them more difficult to control than DC motors [36-44].
Due to their high efficiency and capacity for producing significant amounts of power, AC induction motors are another excellent alternative for producing electricity. However, they need more sophisticated control systems to function well and are frequently more expensive than DC or stepper motors [6]. Here are some of the comparisons for various types of motors.

Table 4:Comparisons for various types of motors

Motor Type	Efficiency	Losses	Advantages	Disadvantages
DC Motors	50-90%	10-50%	Easy to control speed and direction, High torque at low speeds, can be used as a generator in a pinch	Requires brushes that can wear out, needs a controller to regulate voltage and current
DC Coreless Motor	70-85%	15-30%	High power density, Low cogging torque, Low noise and vibration, can be used as a generator	Requires a controller to regulate voltage and current, Lower efficiency compared to brushless DC motors
Brushless DC Motor	85-95%	5-15%	High efficiency, long lifespan, Low maintenance, can be used as a generator	Requires a controller to regulate voltage and current, more expensive than DC motors
AC Induction Motor	85-95%	5-15%	High efficiency, Simple and robust design, Low maintenance	Requires an AC power source, can be more difficult to control speed and direction
Permanent Magnet Synchronous Motor	85-95%	5-15%	High efficiency, High power density, can be used as a generator	Requires a controller to regulate voltage and current, more expensive than AC induction motors

Linear Motor	50-70%	30-50%	Can be used as a generator, Simple and robust design	Limited in terms of power output, Requires precise alignment between the stator and the mover
Stepper Motor	40-60%	40-60%	Precise positioning and control, can be used as a generator	Low efficiency, High torque ripple, Limited maximum speed

The motor selection for a wearable device that reflect on to produce electricity from human motion will depends on several factors, including the motor's size and weight, efficiency, power output, and cost.

As mentioned above, some tiny DC motors are one option to consider because as well, since they are reasonably simple to control and may be made to have great efficiency. There may be a motor that is appropriate for a wearable device because DC motors come in a variety of sizes [4]. Another choice is a stepper motor, which may produce power by turning the motor shaft manually. However, as mentioned above, the stepper motors are complex to control and need additional circuits to convert the output to usable power [6]. Since AC induction motors are extremely efficient and capable of producing large amounts of power, they can also be utilized to produce energy [4]. They may, however, need more sophisticated control systems to function well and are frequently more expensive than DC or stepper motors [6].

The best option of selecting the motor for this project depends on several factors, such as the amount of power that need to generate, space availability, resources budgets etc. Since this project is for wearable options, the DC coreless motors are chosen because of their ease of control and various size availability.

Piezoelectric Discs

The piezoelectric discs are the type of transducers that convert mechanical stress into electrical energy. These transducers are made of quartz and crystals or ceramic that have piezoelectric properties. The structures of these piezoelectric crystals are not symmetrical but exist in an electrically neutral balance. When the mechanical stress is applied to the surface of the crystal, the lattice of the crystal deforms and generate the electrical charge making the crystal to generate electricity. Such effect is called ‘Piezoelectric Effect’ [9]. As for harvesting energy, the piezoelectric discs can be considered as one of the sources to harvest since human can produce many kinds of mechanical stress such as from footsteps by running or walking, punching, and smashing etc. [8] However, in this project the transducers will be used as source from another source’s stress waste which is from magnetic inducing source.

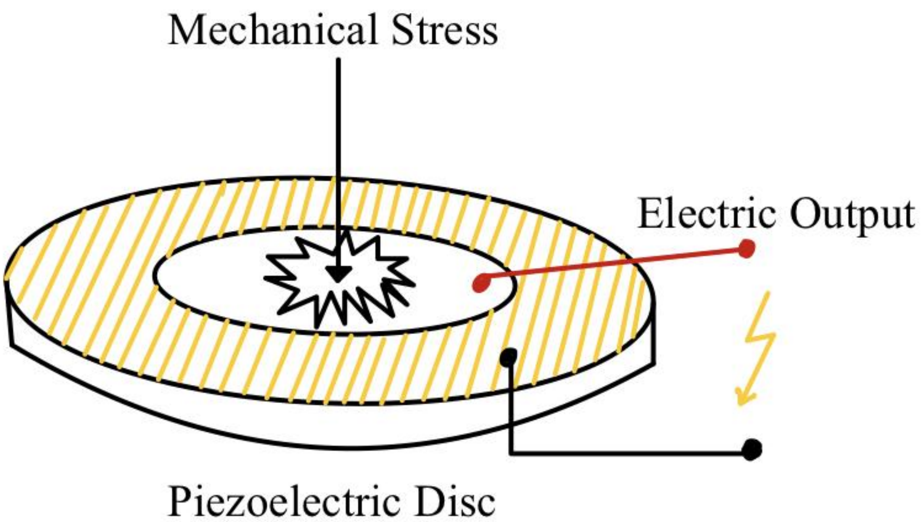

Figure 6 Piezoelectric Disc Diagram

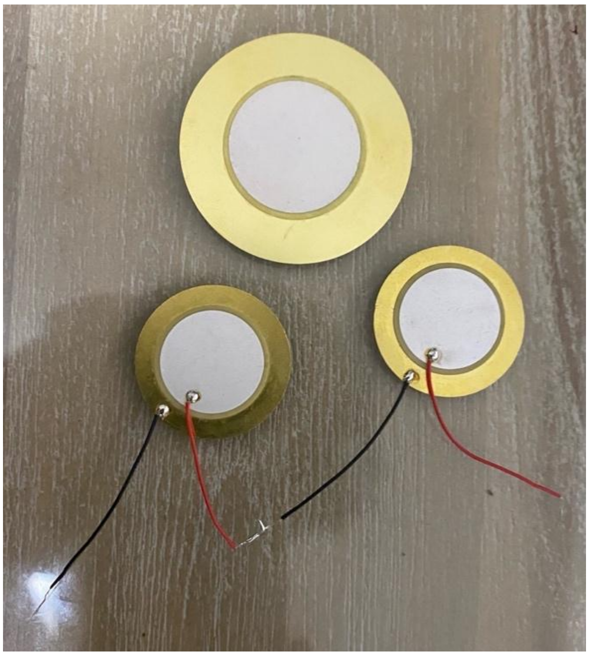

Figure 7: External Diameter 27mm and 41mm Piezoelectric Discs

Piezoelectric transducers are available in various shapes and sizes in the market [9]. As we can see in the above table, the biggest and most power can produce is the oval shaped PZT (Piezoelectric transducer). It can produce around 70V as a spike voltage and current of 250mA. It is also the most efficient of all. However, the oval shaped is not suitable for this project as this will become bulky and will not be fit inside the cylinder. However, for the circular shaped PZT, they already have various sizes, and they can produce fair amount of voltage and current which we will be later used in this project with minimal impact force. Hence, the circular shaped PZT will be apply to this project.

Table 1:Various Piezoelectric Transducers Shaped and Sizes

Shape	Size	Maximum Voltage Produced	Maximum Current Produced	Efficiency	Least Impact Force
Round	10mm	30V	100mA	60%	0.1N
Square	20mm	50V	150mA	70%	0.2N
Circular	15mm	40V	120mA	65%	0.15N
Rectangular	25mmx15mm	60V	200mA	75%	0.25N
Oval	30mmx 20mm	70V	250mA	80%	0.3N
Octagonal	12mm	25V	80mA	55%	0.08N

Electromagnetic Induction

[1] Michael Faraday and Joseph Henry independently discovered the electromagnetism. Ever since that time the electromagnetic induction have been used in many applications such as bicycle dynamo (Alternator), recently back in 2010 from Japan very fascinating shape battery which enable the device without the need for charging the battery itself and some are already manufacturing for wearable devices such as 'Seiko Kinetic Watch'. There are some products like shaking torch which only require the vibration from human without even the need of a battery [7].

As for this project, the design specification of the electromagnetic induction source will mainly be established on the shaking torch. The PVC pipe or acrylic will be used as the handle and housing for the magnetic induction device. The copper coded wire is wind around the middle of the pipe to induce electricity with the magnet. The two-point end of the pipe will be enclosed with the earth rare material neodymium magnet inside and shaken back and forward to produce AC voltage. We can harvest more power form this source. When the device is shaken, the magnet will impact with some force at two ends of the pipe [45-54]. If we replace the two ends with piezoelectric discs, we can harvest more energy from it.

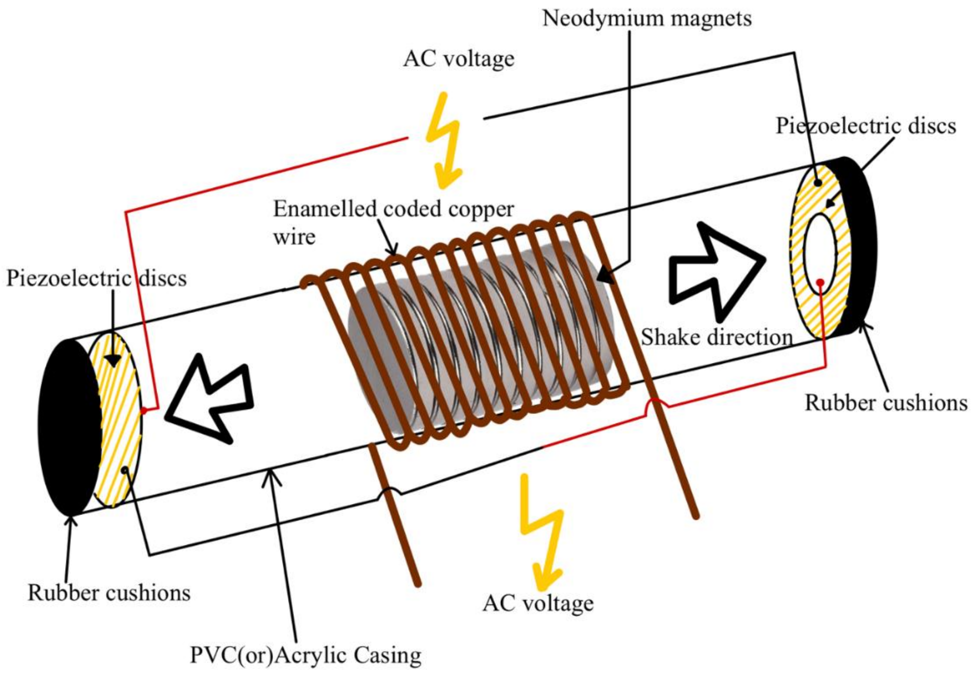

Figure 8: Design Diagram of two combined energy Harvesting systems

The diagram represents that how the combined energy harvesting system will be look alike. By adding the cushions at each end of the shaking energy harvester, we can use it for long terms since the impact force applied on the piezoelectric disc can damage for long term.

There are several products available using this magnetic induction method in the market such as shaking torch, kinetic watch('Seiko') etc. [3]. This method mainly used the Faraday's Law which is:

$$\varepsilon = -N\frac{\Delta \emptyset}{\Delta t} \dots (1)$$

Where ε is electro motive force or EMF, N is the number of turns in the coil, and Ø is the magnetic flux. There is a negative sign due to Lenz's Law

With the above formula, we can break down it further for rate of change in magnetic flux by equation below:

$$\varepsilon = \beta l \upsilon \dots (2)$$

Where β is the magnetic field strength, l is the wire length and υ is the relative velocity between the magnet and the wire. According to the equation (2), we know that we can increase the generated voltage by increasing the flux, length of wire, and velocity. As for designing this project the casing and wires are not hard to choose since they are the fundamental materials. However, choosing the magnet may play major role to this. It is already mentioned in the equation (2) that the more magnetic field or magnetic flux the more voltage it can produce. Therefore, the earth rare neodymium magnets will be used to excite the tube.

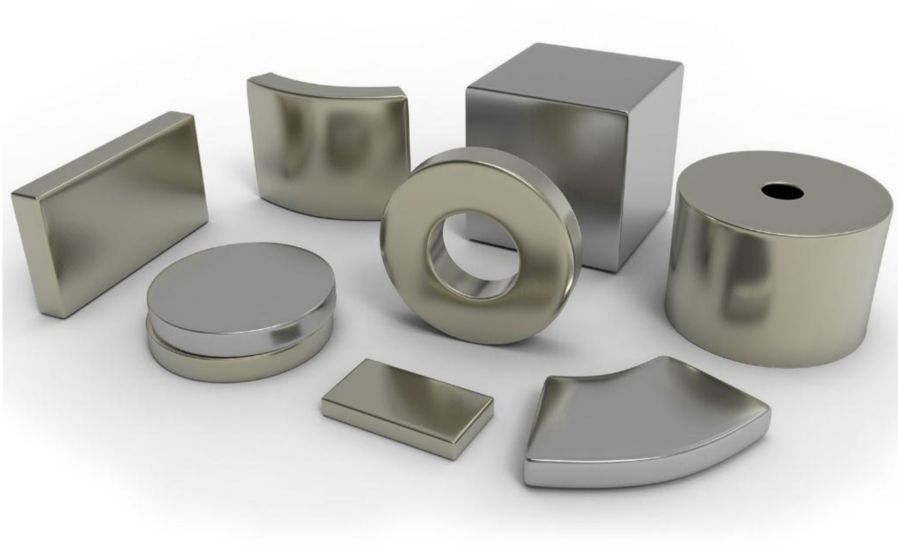

Figure 9: Neodymium Magnets with various shapes [15]

From the above figure, the magnets have various shapes and sizes in the market, the shape must be cylindrical since we are using the casing as the cylinder. However, the magnet field must be specific. the magnetic field of the magnet must be opposed to the wire winding direction as shown from the below figure.

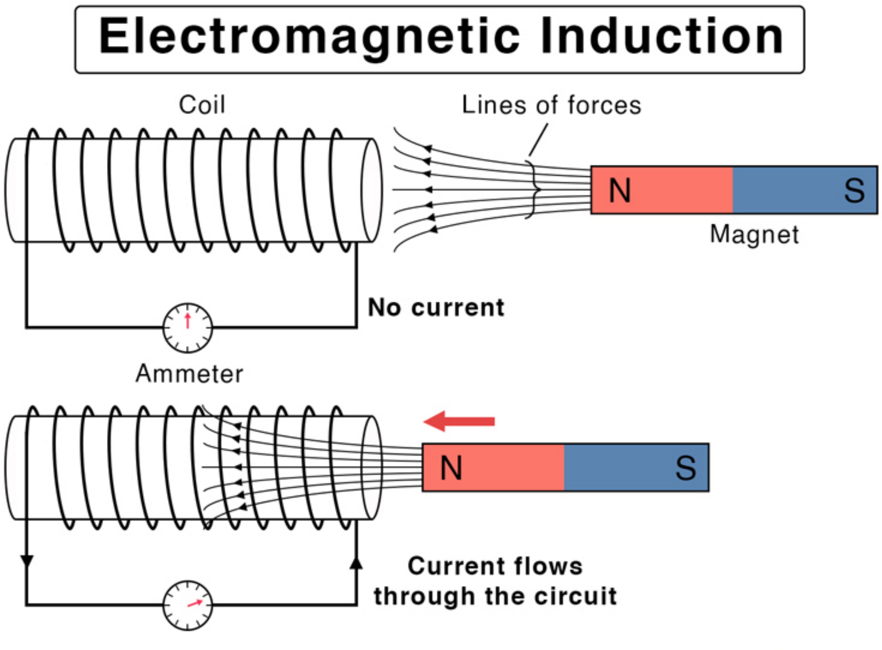

Figure 10: Indication of Electromagnetic Induction [2]

The neodymium magnets are not only strong but also have the highest magnetic flux. It has the flux of 1.0T to 1.4T which is the best option for this project.

IV. OUR APPROACH

First, we must reflect on if the energy harvesting is possible from human body or another source that can harvest energy as the wearable devices. Since human body move a lot during the day and the body produce heat, we can extract energy from movement, heat and solar and even from wind. Hence, we can divide the project into 5 systems, which are:

1. Solar source
2. Wind source
3. Motions source (Electromagnetic induction)

4. Mechanical Stress source and
5. Thermal Source.

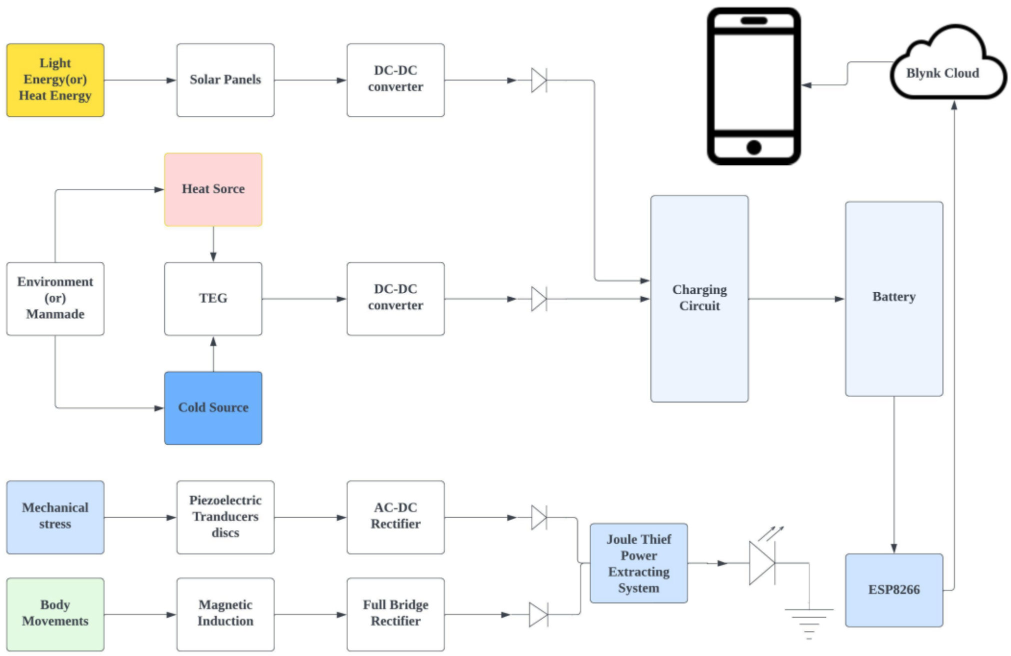

Figure 11: Block Diagram of the Project

According to the above literature reviews, some of the sources are viable and usable for portable applications as for the wearable some harvesting chips are requires as the energy harvested from each of the modules are very small.

V. Feasibility Study

Solar Panel

The main achievement of this project to make all the sources as small as possible so that we can consider them as wearable. As we discussed in the section 4.1, the flexible solar are available to wear however, to build the prototype, the following small panel or similar size will be used since they are portable and can consider them as wearable applications.

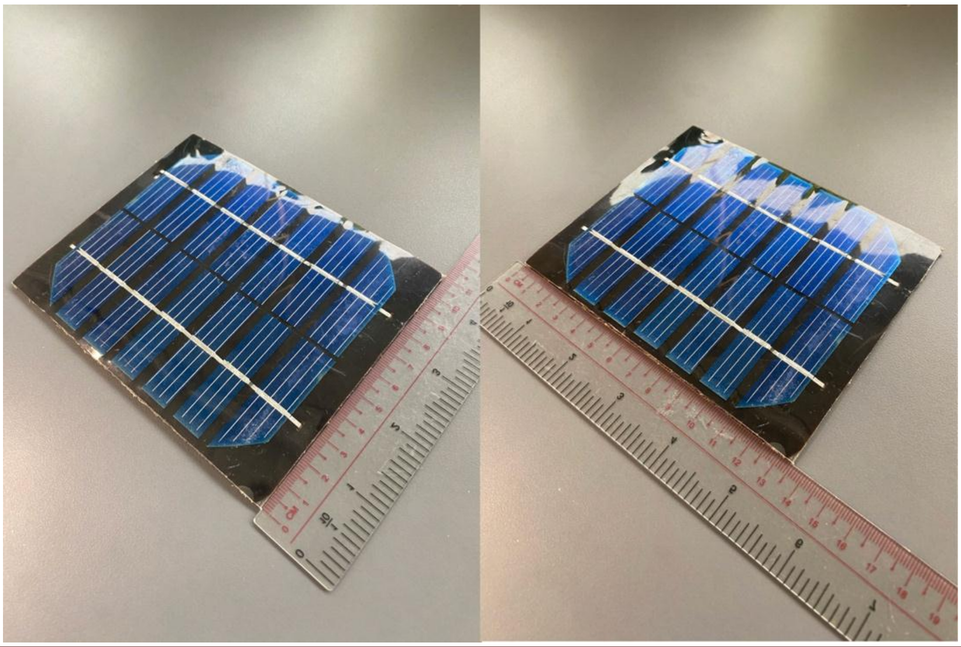

Figure 12: Mini solar panel 13.5cm x 11cm (5V)

The determination of the solar panel's open circuit voltage is tested under the light of the PSB lab. In order to track down the open circuit voltage, the solar panel is connected to the multimeter directly with no load. And give the ambient light intensity as high as possible since it is not easy to get sunlight in the lab which is indoor testing.

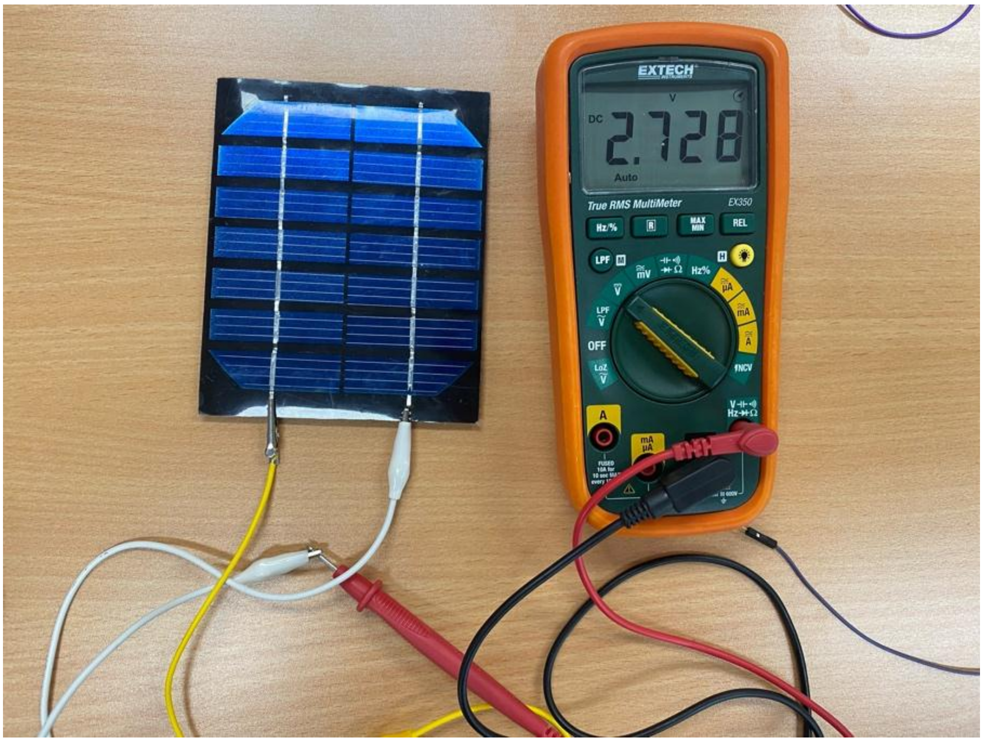

Figure 13: Solar Voc Testing under lab Light

The above figure show that open circuit voltage which is 2.7V(DC) under the light of the lab. However, to get the max open circuit voltage, the panel need the maximum intensity of light. Hence, I put the solar panel under the lamp as close as possible to get the max open circuit voltage.

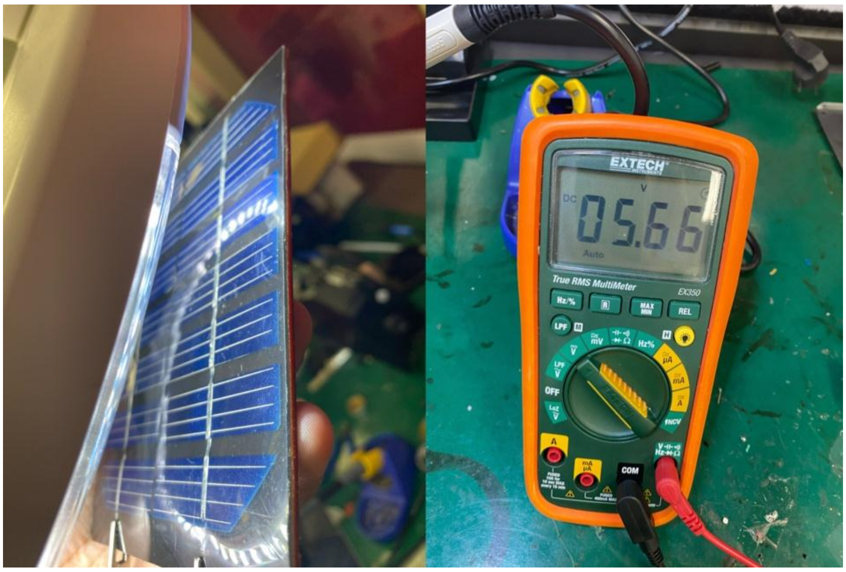

Figure 14: Open circuit voltage under lamp light (5cm apart)

As we can see from the figure 13, we can get the maximum open circuit voltage by putting the lamp and which is considered to be around 5cm apart. The short circuit current that I measured with different distance apart are in the table 6.

Table 6:Different Distance to the Voc and Isc

No.	Distance between Solar and the lamp	Open circuit Voltage	Short circuit current
1.	5cm	5.65V	2.9mA
2.	18cm	5V	1.7mA
3.	34cm	4V	0.79mA
4.	67cm	3.3V	0.36mA

Figure 15: Voc and Isc measurement (18cm apart)

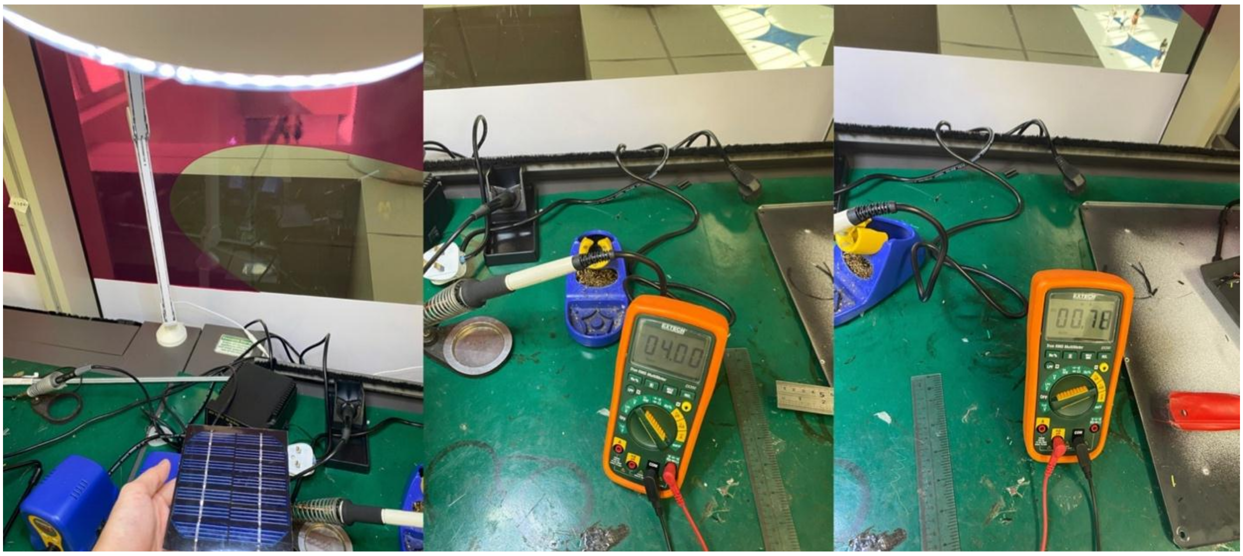

Figure 16: Voc and Isc measurement (34cm apart)

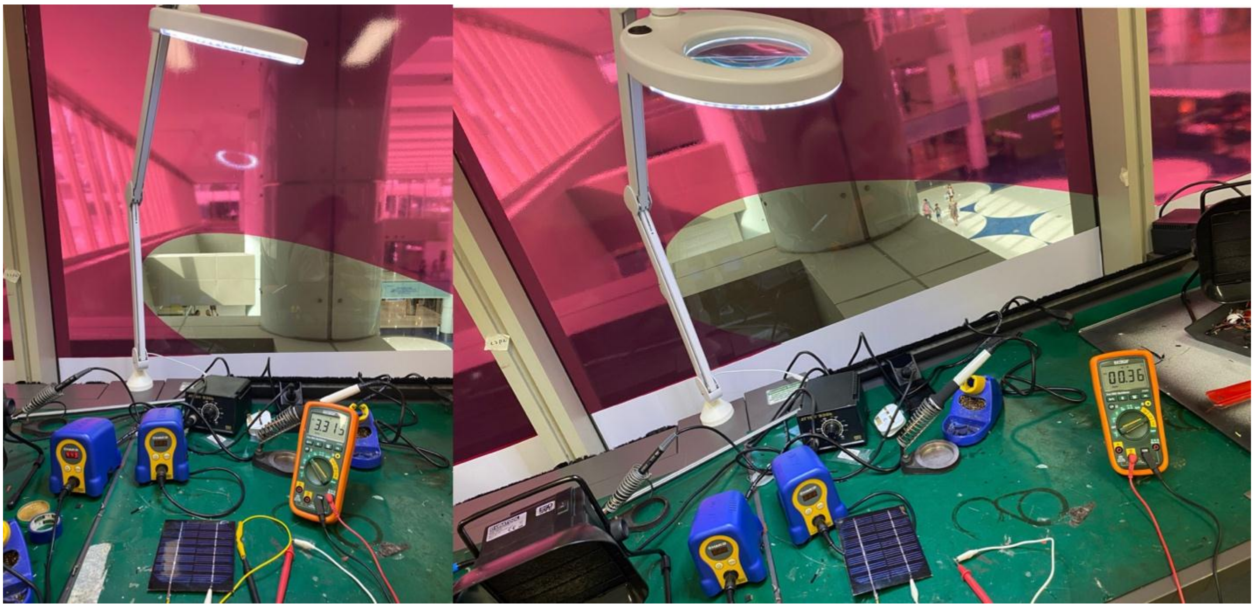

Figure 17: Voc and Isc measurement(67cm)

After that we will be testing the current by connecting with the potentiometer or variable resistor. The results are as below. In this manner we can get the Voltage at maximum power.

Table 7:Current and voltage with different load (38-40cm± 1cm distance)

No.	Resistance(Ω)	Current(µA)	Voltage(V)
1.	1000Ω	820	0.82
2.	750Ω	832	0.624
3.	500Ω	848	0.424
4.	250Ω	862	0.2155
5.	0Ω	875	-

Since the Voltage and current gain is very low I will reduce the distance between the solar panel and lamp in other word increasing the light intensity.

Table 8:Current and voltage with different load (17cm± 1cm distance)

No.	Resistance(Ω)	Current(mA)	Voltage(V)
1.	1000Ω	2.2	2.2
2.	750Ω	2.22	1.665
3.	500Ω	2.26	1.13
4.	250Ω	2.3	0.575
5.	0Ω	2.36	-

The current measurement with different load test under two different distance apart 40cm and 17cm. The figures are as below.

Figure 28: Current measurement with 1kΩ Load from 40cm apart

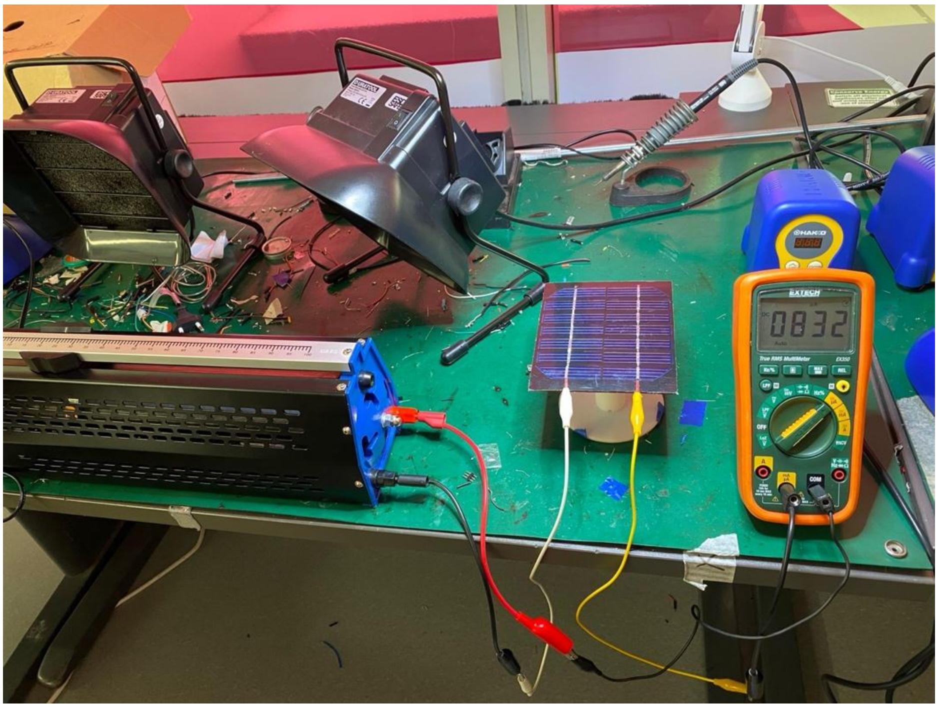

Figure 19: Current Measurement with 750Ω load

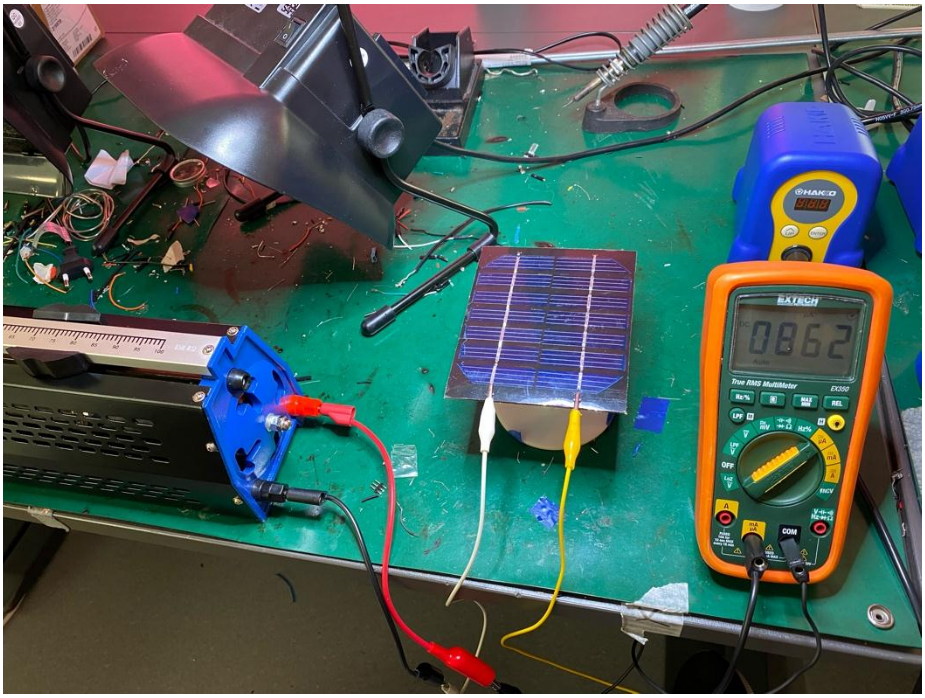

Figure 20: Current measurement with 500Ω Load

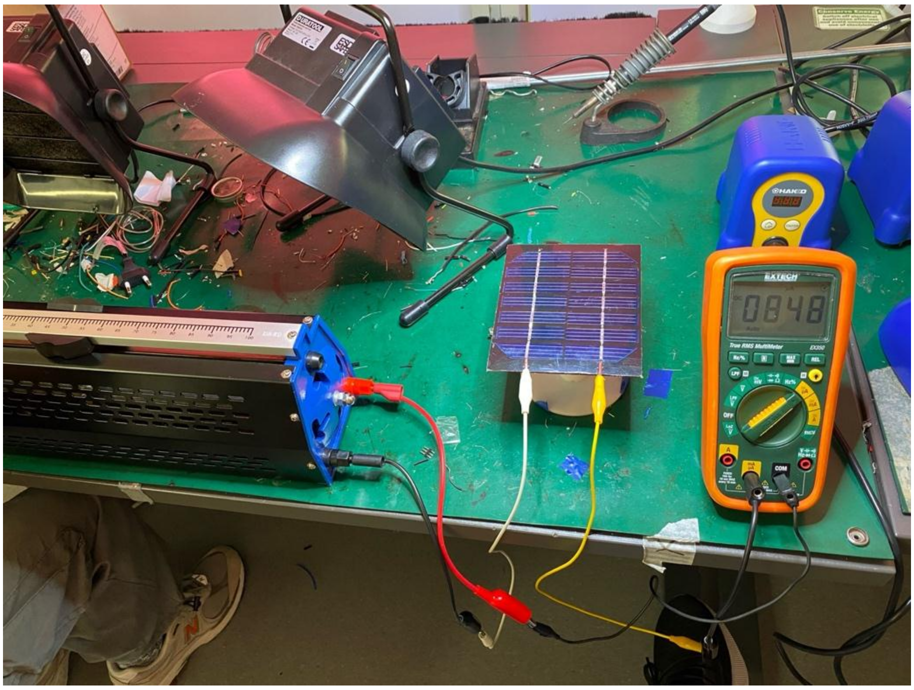

Figure 21: Current Measurement with 250Ω Load

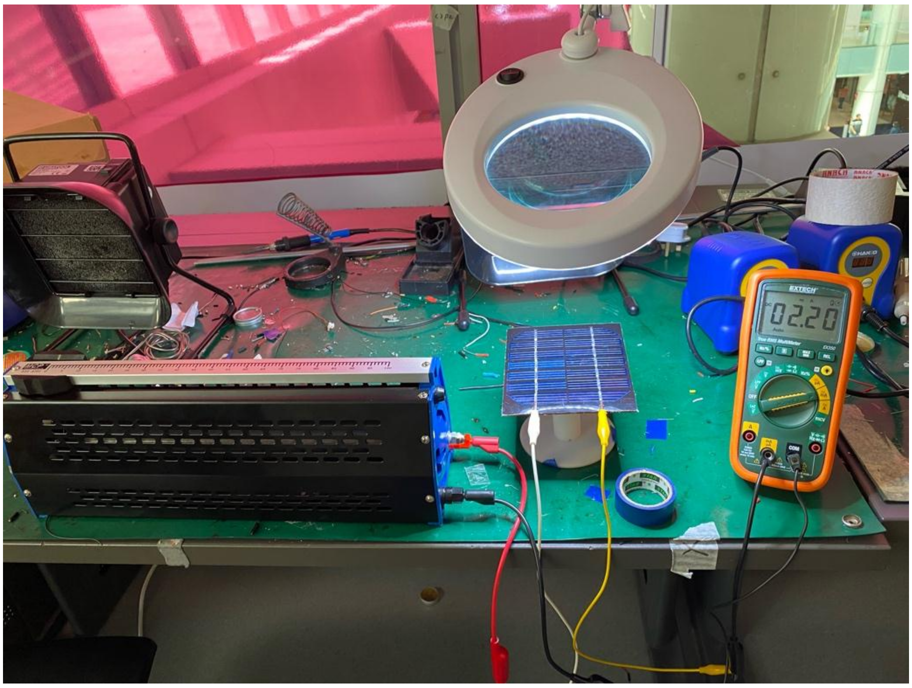

Figure 22: Current measurement with no load 0Ω

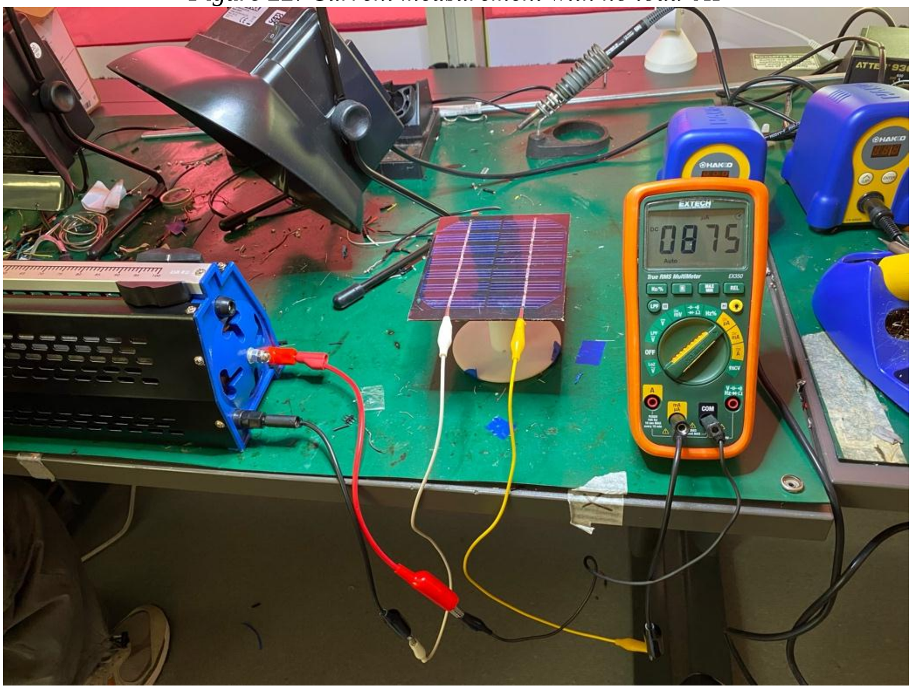

Figure 23: Maximum current measurement with 1kΩ Load from 17cm apart

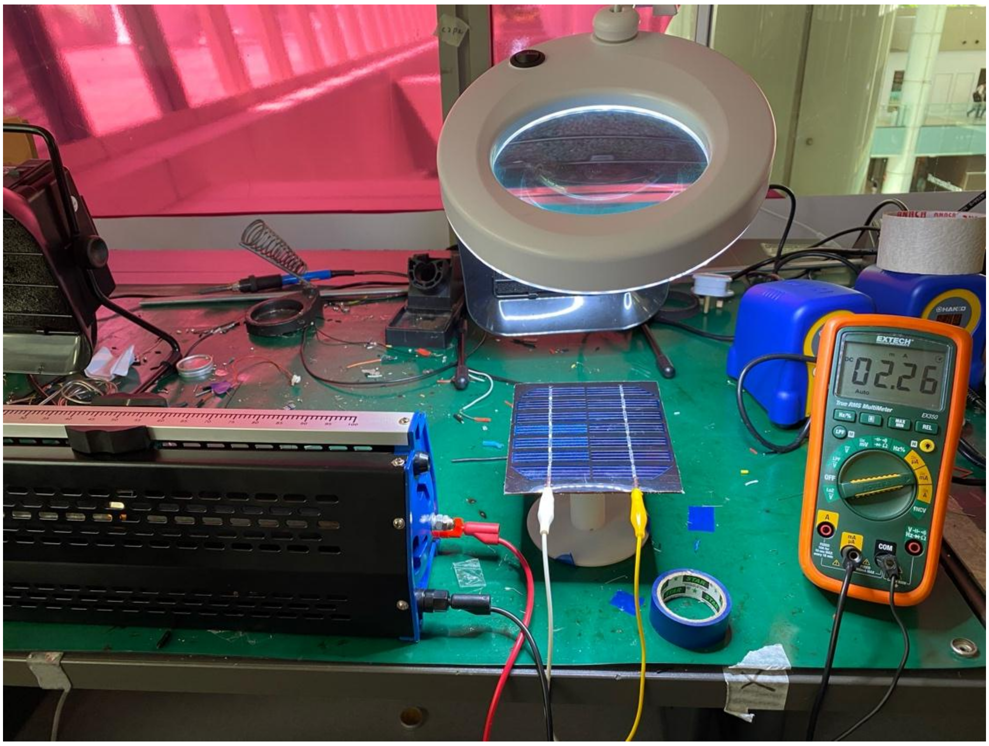

Figure 24: Current Measurement with 750Ω load

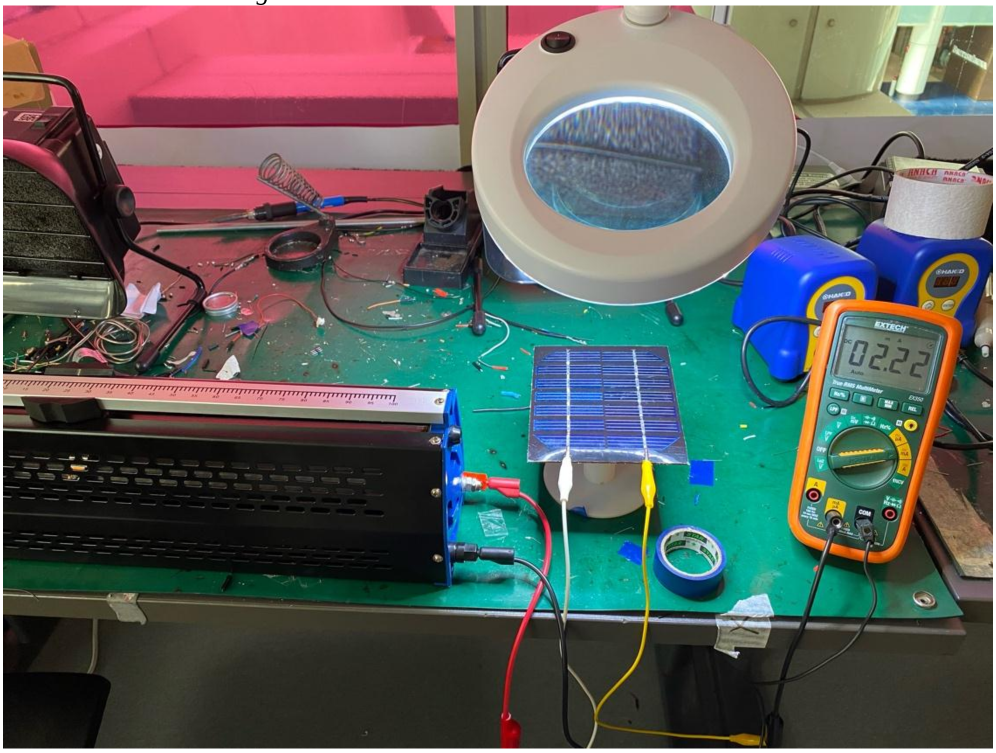

Figure 25:Maximum Current Measurement with 500Ω load

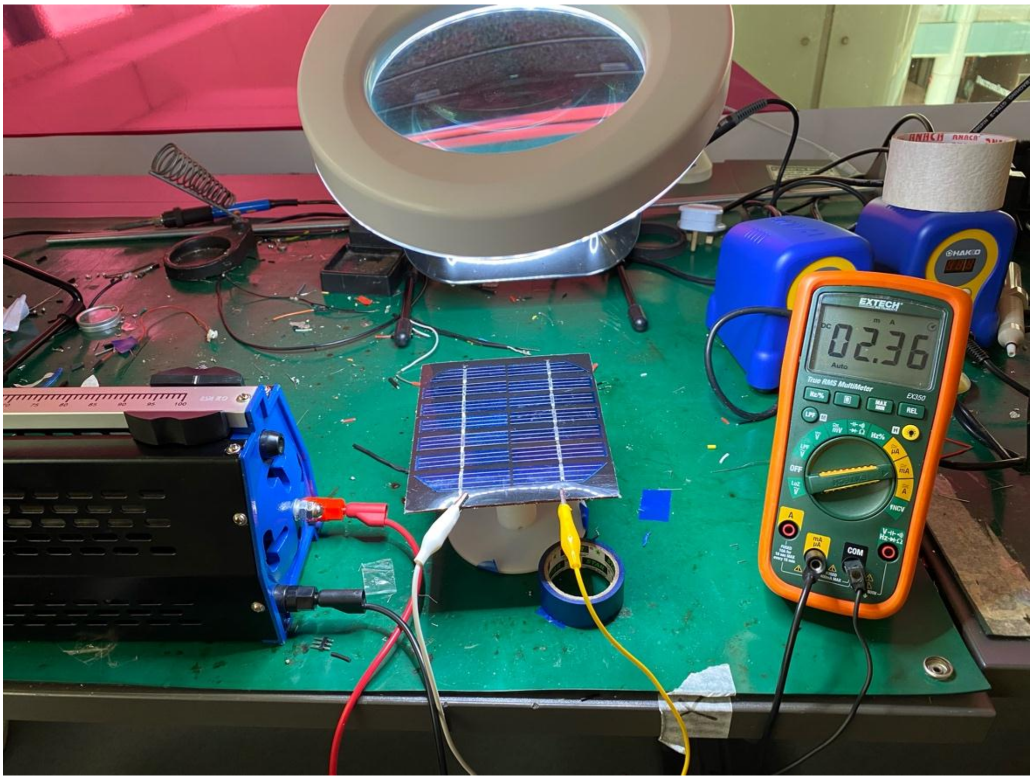

Figure 26: Maximum Current measurement with 250Ω load

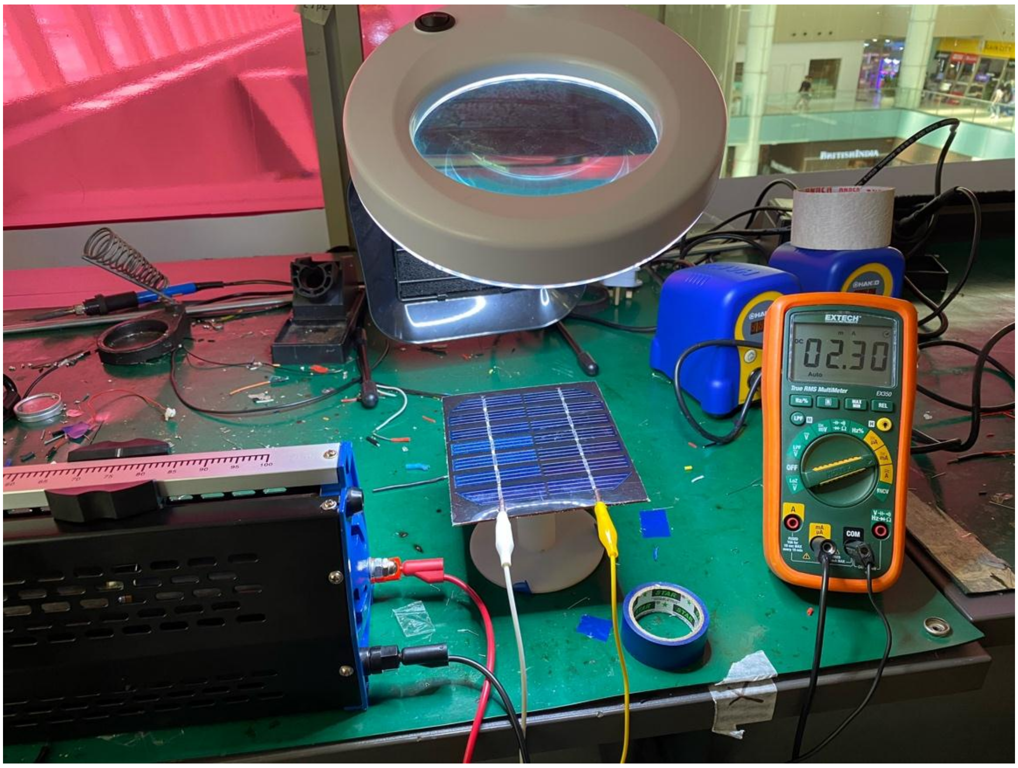

Figure 27: Maximum current Measurement no load

Estimated calculations on TEG modules or Thermal Electric Generators

The key point of extracting the energy form TEG module is to find the great temperature different. In other words, the greater the temperature different the better voltage and current it can generate. It is already mentioned in the table 6. However, from human body heat and ambient temperature is relatively low, Hence, the voltage and current output is expected to be very low. The generated Voltage can be estimated by the following formula:[13]

$$V = S \times \Delta T$$

Where S is the Seebeck coefficient and ΔT is the differential of the temperature.
Since the health human have the temperature of around 37°C and the room temperature have around 30°C. and assuming the Seebeck coefficient is 200μV/K (from table 6). The Temperature different ΔT is

$$\Delta T = 37℃ - 30℃ = 280.15K$$

Hence, the voltage will be:

$$V = 200\mu V/K \times 280.15K = 56.03 \times 10^{-3}V = 56.03mV$$

With, 1kΩ load,

$$I = \frac{V}{R_{load}} = \frac{56.03mV}{1k\Omega} = 56.03\mu A$$

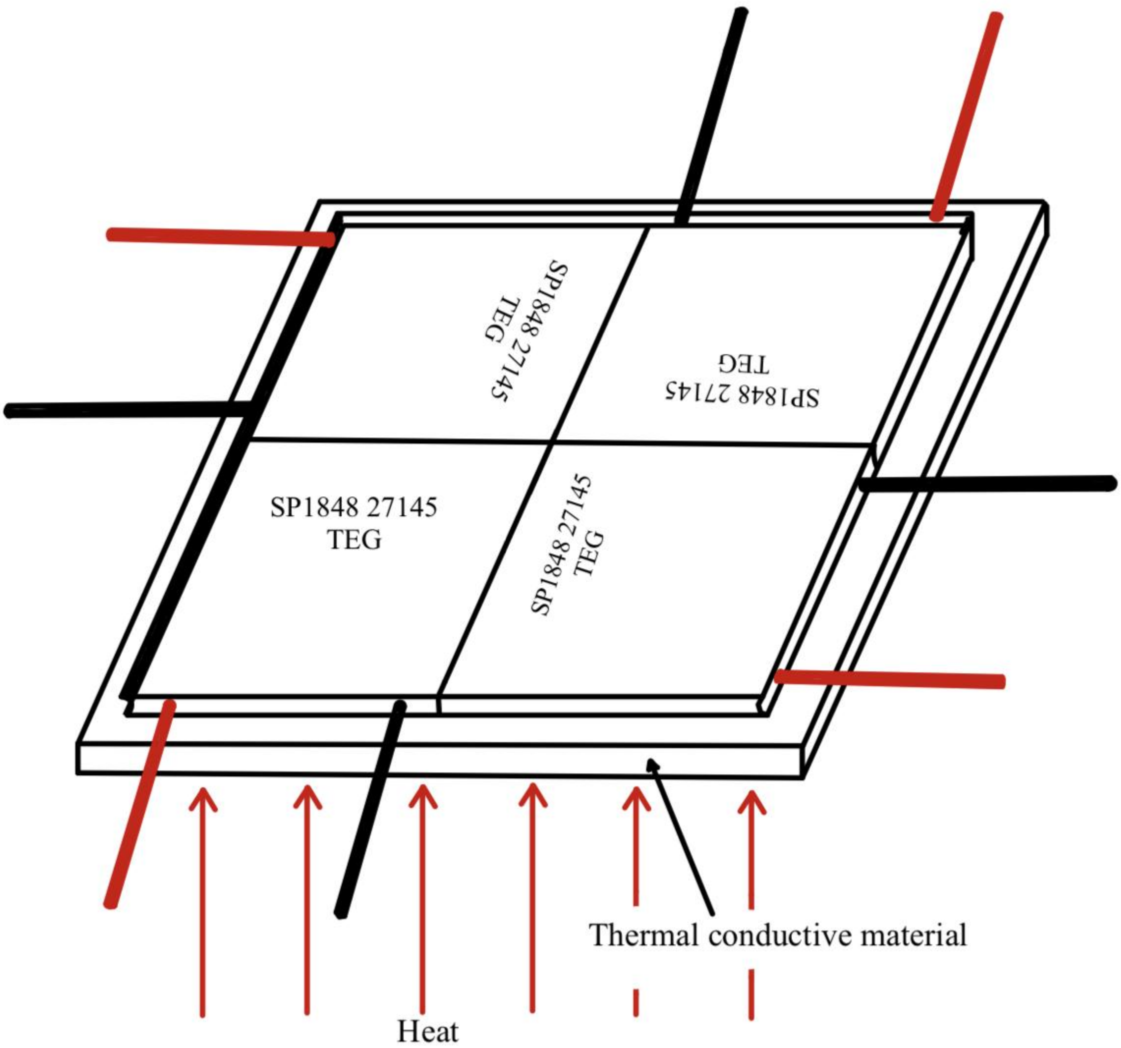

Figure 28: TEG Prototype Design & orientation

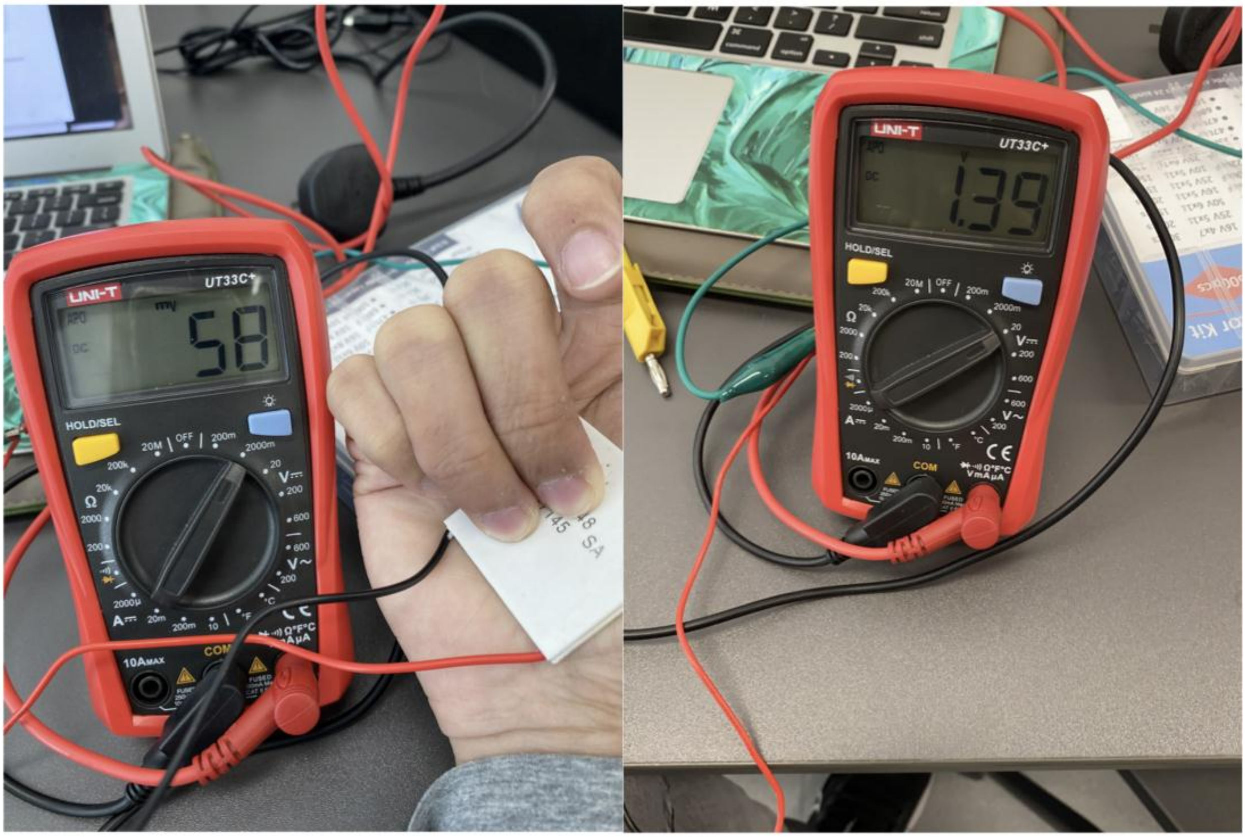

Figure 29: Voltage output from palm temperature and fire

The figure (34) represents that the voltage output from Seebeck effect which generated from the palm heat and fire. The ambient temperature of the lab is assumed to be around 29°C since the experiment is performed in the lab. The maximum voltage output from one module with the lighter fire temperature and ambient temperature is 1.39V. According to the above picture we can see that the voltage generated from the palm heat is close to the calculation which is 56mV from theoretical calculation and 58mV from the practical testing.
If we can further increase the temperature different by adding the heat sink to the cold side, we can get harvest more power.

Magnetic Induction estimated calculations and design configurations

There are many factors that need to consider when building the magnetic induction source. The major things need to consider are, the number of turns of the wire, flux density, and the frequency of oscillation from the human [12]. We can determine the number of turns by assuming some of the factors. Based on my design, I am using the 16cm long clear acrylic pipe as the casing for the harvesting device. The outer diameter will be 20mm and the wire diameter of 0.5mm. If we want to get around 4.5Vp-p, the number of turns can be calculated by:

$$N = \frac{V_{p-p}}{K \times B_{max} \times A \times f}$$

Where, K is he fill factor for cylindrical coil, B_{max} is the maximum flux density, A is the area of the coil, and f is the oscillation frequency. First, the cross-sectional area of the coil as:

$$A = \pi r^2 = \pi\left(\frac{20mm(pipe\ diameter) - 0.5mm(wire\ diameter)}{2}\right)^2$$

$$A = 2.986 \times 10^{-4} m^2$$

The oscillation frequency as 15Hz because it is the consider that the healthy human can generate or shake the device and the magnetic flux as 1.4T since we are using the neodymium magnet. The fill factor K is assumed to be 0.4. Hence, from that, we get the number of turns by:

$$N = \frac{V_{p-p}}{K \times B_{max} \times A \times f} = \frac{4.5}{0.4 \times 1.4 \times 2.986 \times 10^{-4} \times 15}$$

$$N = 1794.08 \approx 1794 Turns$$

The Inductance of the coil can be estimated by:

$$L = \frac{N^2 A\mu}{l} (\mu = permeability\ of\ the\ air)$$

$$L = \frac{1794.08^2 \times 2.986 \times 10^{-4} \times 4\pi \times^{-7}}{0.03(length\ of\ the\ winding)} = 40.259mH$$

These calculations are assumed by some close factors and the real-life output can be different. The design configuration will be shown in the below figure.

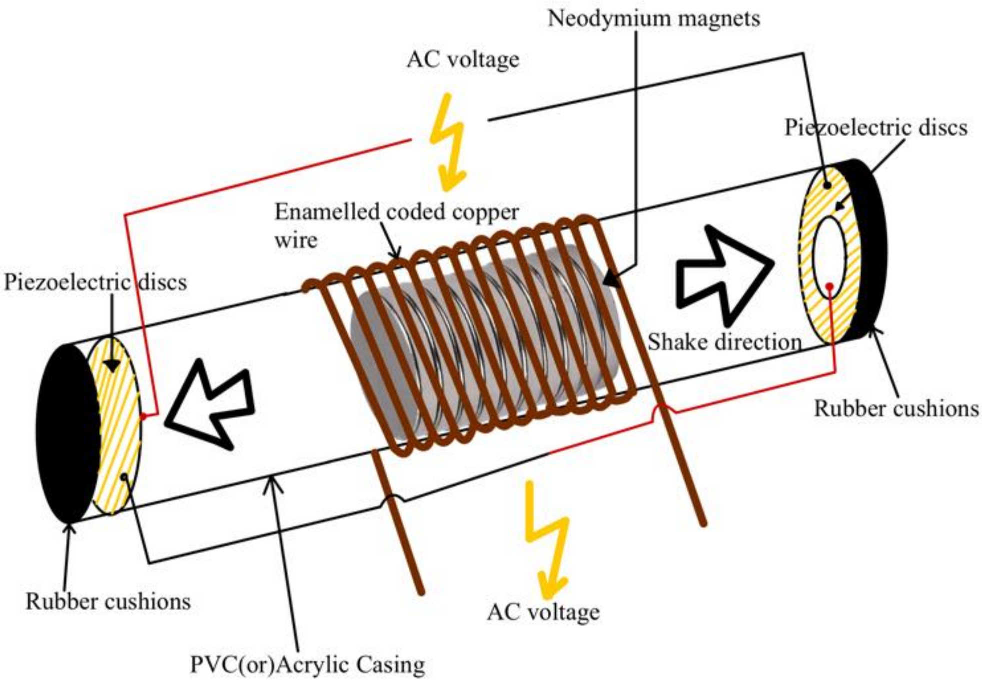

Figure 30: Design Configuration of magnetic induction

The impact force of the 10 magnets to the piezoelectric can be calculate by the above parameters of the vibration source. I am using 10magnets which have 3mm thickness making them 30mm thickness for the whole magnet. The impact force can be calculated by this formula.

$$F = Mass \times Accelatation$$

$$Accelaration = \frac{2 \times distance}{T^2}$$

The distance travel for the magnet is $l(casing) - magnet\ thickness = 160mm - 30mm = 130mm$

$$\therefore Accelaration = \frac{2 \times distance}{T^2} = \frac{2 \times distance}{\frac{1}{f}^2} = \frac{2 \times 130mm}{(\frac{1}{15})^2} = 57.91m/s^2$$

$$For\ the\ mass = density \times Volume = \rho \times \pi r^2 h$$

Since the magnet have density of 7500kg/m^3 and diameter of 15mm,

$$mass = 7500 \times 5.3 \times 10^{-7} = 0.00397kg$$

$$Hence, F = Mass \times Accelatation = 0.00397kg \times 57.91m/s^2$$

$$\therefore F = 0.22N$$

This impact force is the force that each time it will hit the piezoelectric to the magnet.

The output of the magnetic induction device is also AC output .Hence, the output is connected with the full bridge rectifier the connected to the self-oscillating circuit (or) joule thief circuit to boost up the voltage. The circuit diagram is as below:

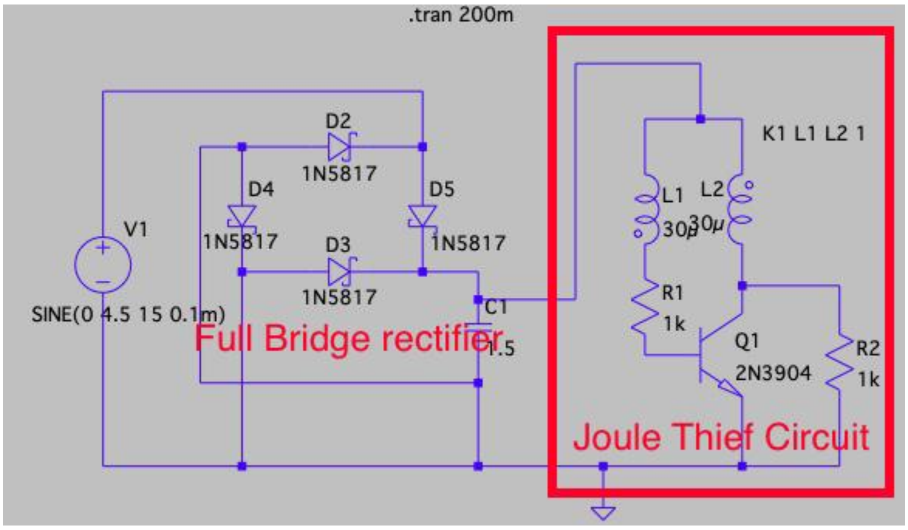

Figure 31: Circuit diagram of the magnetic induction energy harvester

Working Principle and application of Joule Thief Circuit

Joule Thief circuit or self-oscillating circuit is a voltage booster circuit that converts the constant low voltage into higher periodic voltage. This circuit is mostly applied in low voltages sources and very useful in extracting the maximum amount of energy;/ in a period from energy storage like batteries and super capacitors. Hence this circuit will be used in emergency use for extracting the maximum amount of energy from the battery.

Working principle

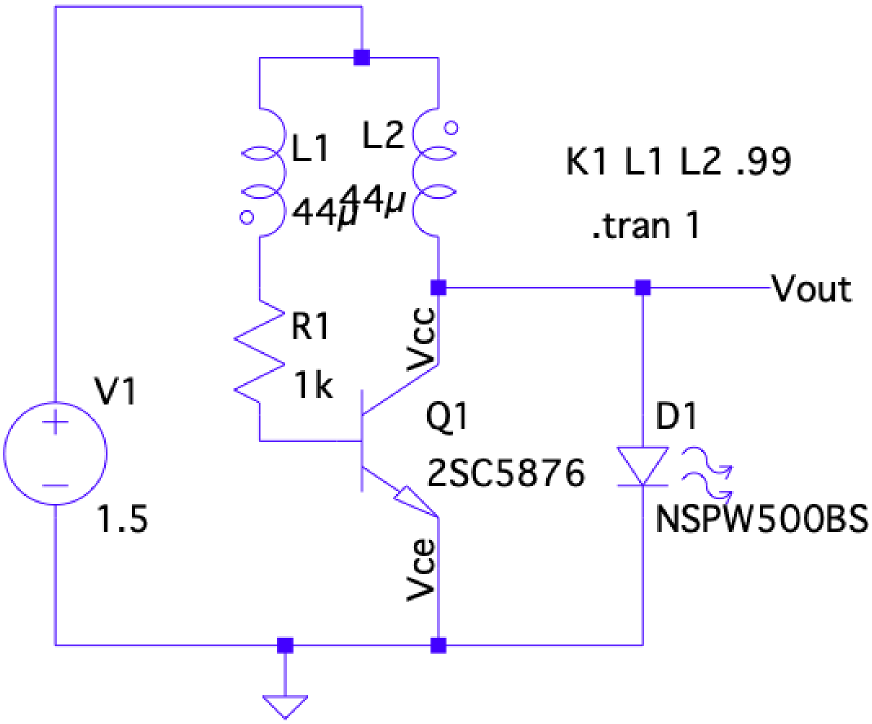

Figure 32: Emergency Power extraction circuit or Joule Thief Circuit

The circuit in this project include NPN transistor, resistor, and a hand winded transformer which created by winding the Enamel copper wire around the ferrite toroid core. The circuit schematic is shown in the figure (40). At first a small amount of base current only let the small amount of collector current to flow. This collector current induces the voltage to the secondary coil of the transformer in this case L1. This secondary coil is connected in series with the source and due to its reverse winding direction thus increase the base current which also increase the collector current. This process repeats until the transistor reach its saturation state.

The collector current rise in a linear fashion and the primary coil of the transformer builds up the magnetic field gradually increase the magnetic flux density of the toroid coil to its maximum state. Once it the flux density of the toroid coil reach the maximum state the induce voltage decrease and the base current decreases as well and the transistor is no longer in a saturation state hence making the collector current cannot flow anymore. However, the energy of the magnetic field in the primary coil need to dissipate and thus making the voltage output very high at Vout. According to "instructible" [17] if no load is connected the output voltage can be as high as 60 to 94V and the minimum operating voltage of this circuit is 0.4V.

Simulation and Practical Results

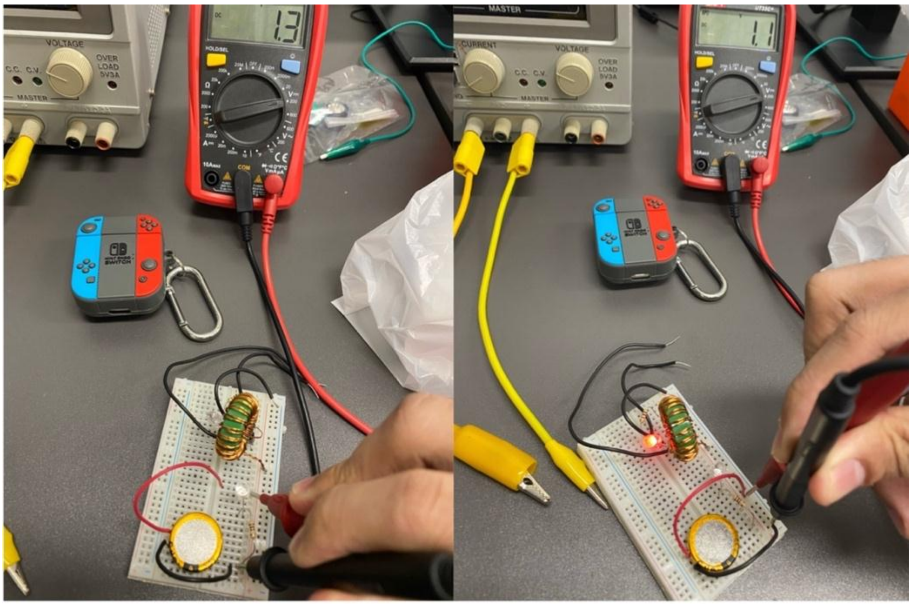

Figure 33: Start Up voltage of Joule Thief Circuit (0.4V)

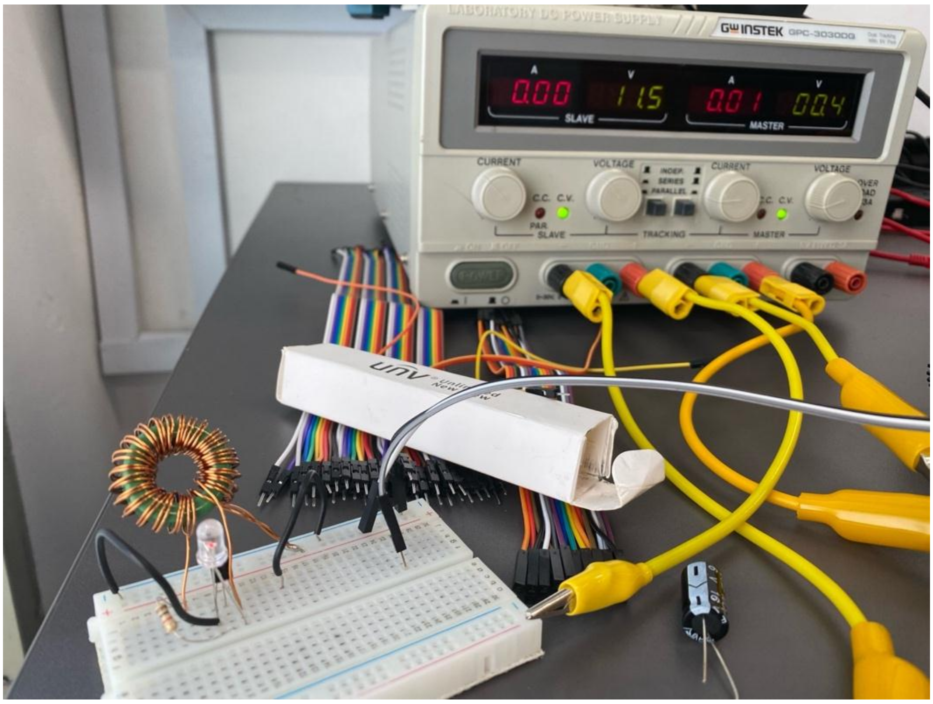

Figure 34: Unused Voltage Testing from Super capacitor with & without Joule Thief circuit

The supercapacitor in this result is 1F and 5.5V. As seen from the above figure (42) the LED turn off while the capacitor still has a charge of 1.3V. However, with Joule thief circuit, the LED is brighter and still illuminating for around 20min. We can calculate the unused energy by the following formula:

$$E_{1F(before\ LED)} = \frac{1}{2} \times C \times V^2 = \frac{1}{2} \times 1F \times 5.5^2 = 15\ J$$

$$E_{1F(After\ LED)} = \frac{1}{2} \times C \times V^2 = \frac{1}{2} \times 1F \times 1.3^2 = 0.845\ J$$

Hence the unused energy is:

$$Unused\ Joule = \frac{0.845J}{15J} = 0.0563 = 5.6\%$$

Therefore 5.6% of energy is unused in the supercapacitor without the joule thief circuit. By using the circuit, we can extract the maximum amount of energy from the battery or a supercapacitor. The results of the simulation and practical results are as below.

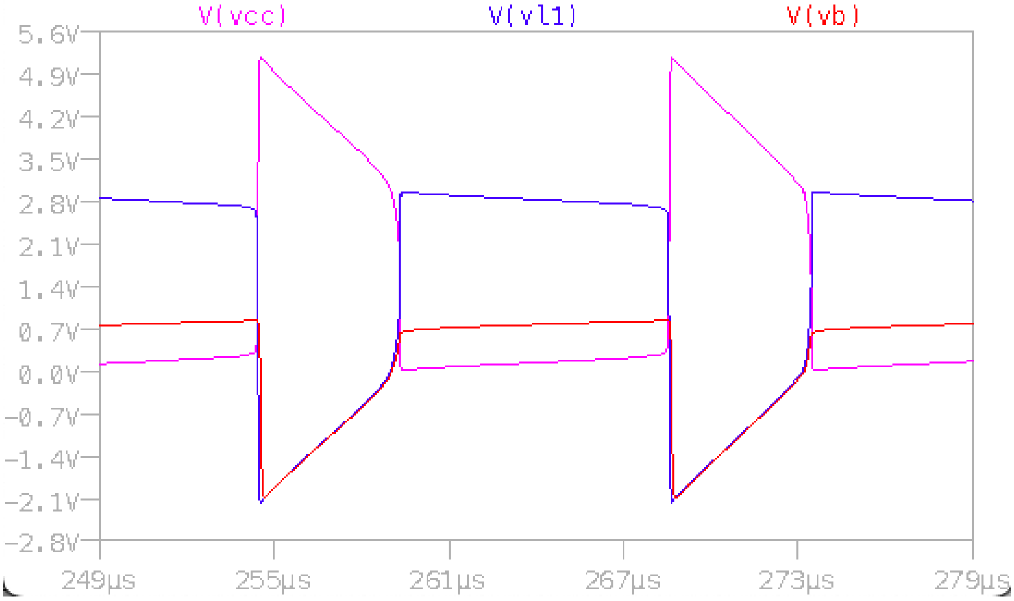

Figure 35: Joule Thief Circuit Vc, Vb and VL(Simulation)

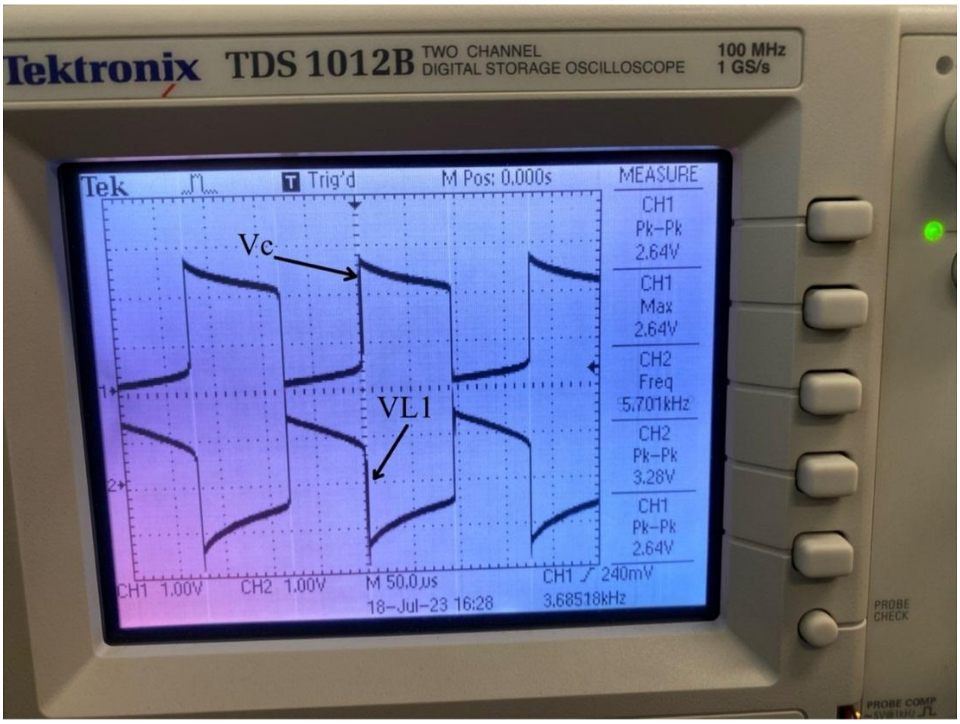

Figure 36: Joule Thief circuit Vc and VL (Practical Result)

Discussion

According to the above two results from practical and simulation, the two results are close to each other. By the wave form of the two results, they are similar to an oscillator which act like a boost converter. We can also see the charging and discharging in the secondary coil of the transformer. At some point of voltage which is around 3.5V-4.5V the frequency increase as well and the oscillation disappear completely. In order to solve this, we can increase the inductance of the transformer by winding the bigger toroid coil and thus slow down the charging and discharging process decreasing the overall frequency of the oscillator, or we can increase the value of the base resistor which decrease the overall base current.
Furthermore, we can make it as a charging circuit by adding capacitor to the node between resistor and secondary coil to stabilize the output adding Zener diode to the base help prevent the damage by voltage spikes to the transistor and add the diode across the battery to the primary to prevent the battery from draining back to the transistor.

VI. IoT Application

The IoT platform which will be used in the project is Blynk Platform. The Blynk cloud provide the server infrastructure which is responsible for binding the whole platform. This contains the iOS and Android and web dashboard which allow the user to monitor or adjust the designed applications via web browser.
In this project the IoT platform is used to monitor the battery capacity percentage left and inform the user to change the source to emergency power extracting system if the battery percentage is at critical state while constantly showing the battery capacity and power extracted from the source.
The MCU for this platform is ESP8266 development board which include 17GPIO pins, UART communications, SPI, PWM, ADC, 2.4Ghz WIFI and many other features. In addition, it only needs 3.3V with 5V tolerant and it only draw 12mA of current which is considered as low powered processor can be used in many wearable and portable applications.

<u>Components</u>

Microcontroller
The project is about energy harvesting for portable applications hence IoT is applied as a load for some sources which can provide enough power to it. The IoT have variety of applications such as smart home, smart wearables, smart cars, smart farming, smart retail, smart cares etc. In the project the IoT technology will monitor the battery voltage and capacity and display on the mobile devices. In addition, the humidity and temperature of the environment on the small OLED display.
The chosen MCU have integrated Wi-Fi which allow the user to easily connect with internet and other Wi-Fi capability devices. This alone makes them ideal for the IoT applications and projects. Having a reasonable price and compact design is also the reason for this project application. It also supports the MQTT also known as message queuing Telemetry Transport enabling the system efficient and reliable communication between the IoT device and cloud platforms.

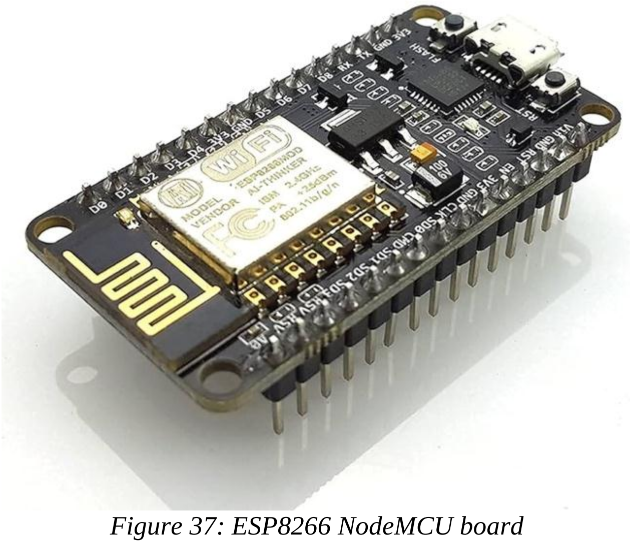

Figure 37: ESP8266 NodeMCU board

Humidity sensor

The MCU chosen do not have the built in humidity and temperature which require the external sensor for this project. DHT22 AM2302 temperature and humidity sensor is used in the IoT application. This sensor will send new data every second and it operate Voltage is 3.3V to 5V which is suitable for low power consumption applications. The accuracy for temperature is ± 0.5°C and the humidity accuracy is ± 2%.

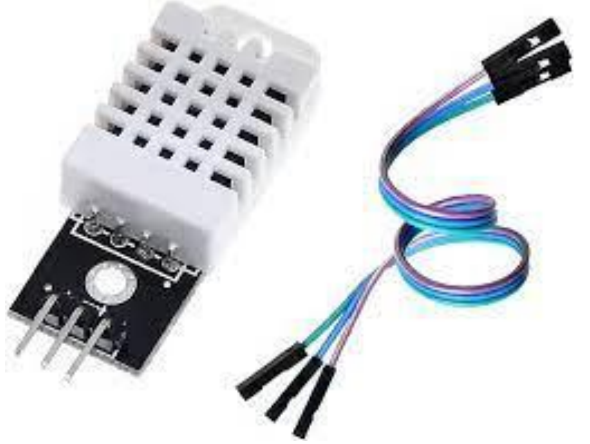

Figure 38: DHT22 AM2302

Display

The display in the application of IoT is used for showing the temperature and humidity of the environment. This display operates at 3V-5V which is good choice low energy consumption applications. It has a resolution of 128 x 64 and the display is white on black background.

Figure 39: 128x64 pixel OLED display

Battery

Energy harvesting is about harvesting energy from the various sources and storing the harvested energy. The battery become the essential part in storing the harvested energy in this project. The most noticeable battery they used in IoT project are Li-ion and Li-Po batteries due to its large capacity and various sizes. However, both have their own advantages and disadvantages. In this project li-ion battery is applied to store power due to having the high-power density, lack of memory effects (when battery become harder to charge over time), and significantly lower cost than Li-Po batteries. In this project 3.7V Li-ion which is enough power for the Battery monitor and humidity sensing IoT application.

Li-ion charging and protection IC

The battery that is chose for this project is Li-ion. Using such battery can be very suitable for energy harvesting devices yet can be dangerous as well. Due to its nature of explosion when overcharges, the proper charging IC and protection circuit is necessary. TP4056 charging and protection IC is used in this project. This IC have a charging and protecting circuit integrated on one IC. However, the IC cannot charge and provide load at the same time. Hence the IRF4905PBF MOSFET is connected at the output of the IC allowing it to charge and provide the load at the same time with the IC.

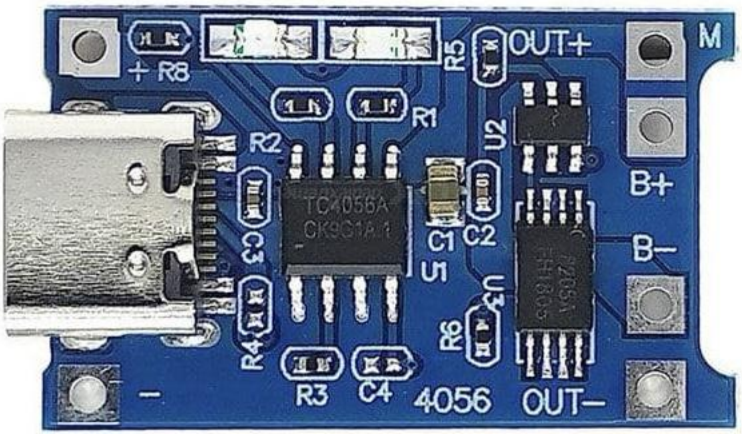

Figure 40: TP4056 Li-ion Charging and Protection IC

IoT working principle with energy harvesting.

The components chosen in this project are low power components which is 3.3 to 4V. If the harvesting source can provide enough power, we can extend the performance of the IoT by providing power to the device directly while the battery is charging. However, as the battery charging IC mentioned above cannot charge and provide load as the same time. Hence the IRF4905PBF MOSFET is connected at the output of the IC as the load sharing circuit, allowing it to charge and provide the load at the same time with the IC.

Therefore, if the source is solar, solar panel will provide power during the daytime or sunny day while charging the battery and when the source cannot provide enough power, the battery will provide during nighttime. In addition, for the IoT device the voltage divider circuit is applied to monitor the battery voltage and capacity of the battery. All of the data such as temperature, humidity battery voltage and battery percentage will send through the cloud which can monitor through mobile devices. If the battery is fall below 3V the notification will send through the connected devices informing the user to charge the battery.

VII. IMPLEMENTATION OF PROPOSED WORK

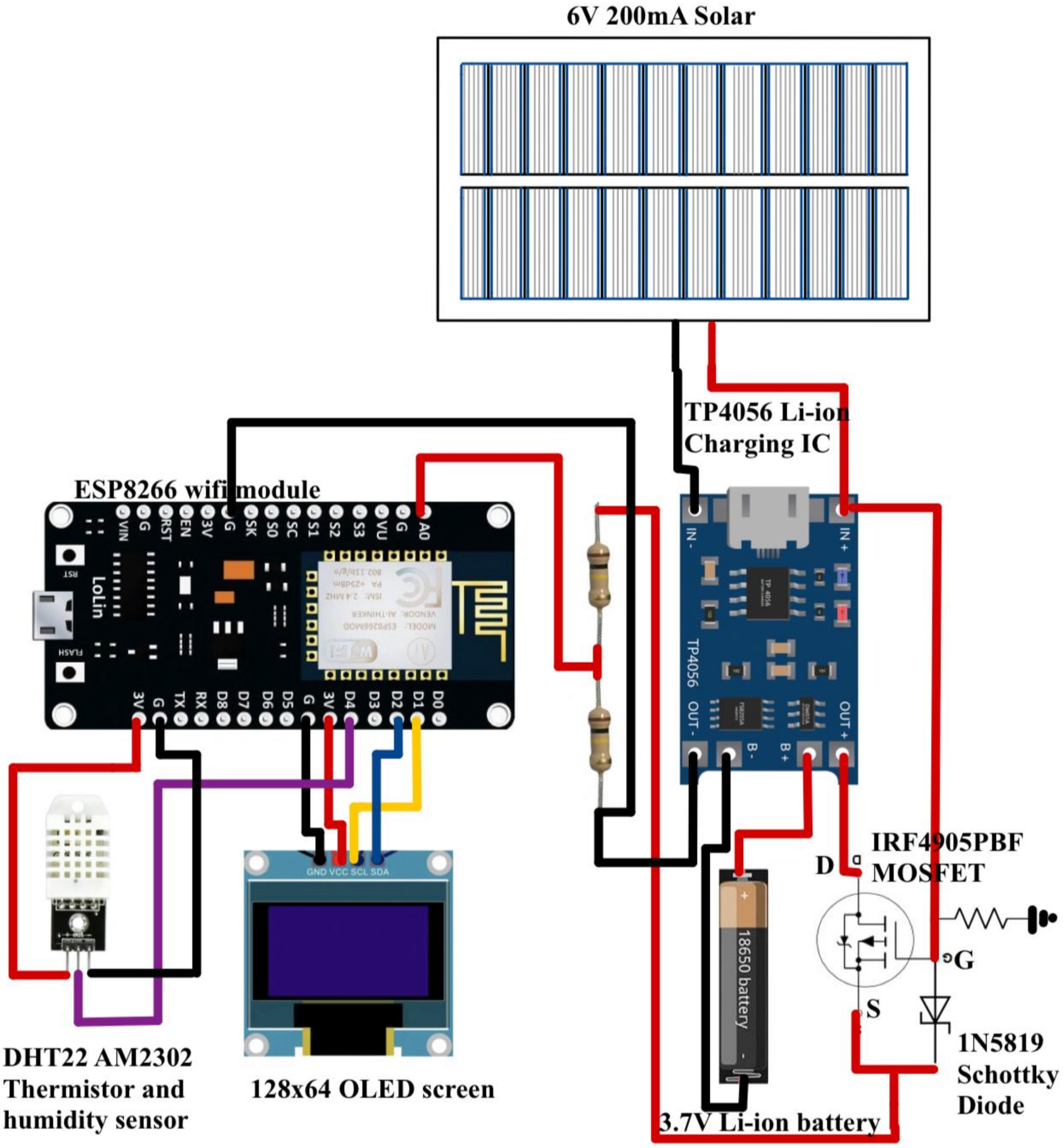

Figure 41: Solar Energy harvesting for IoT application.

Current consumption of the IoT

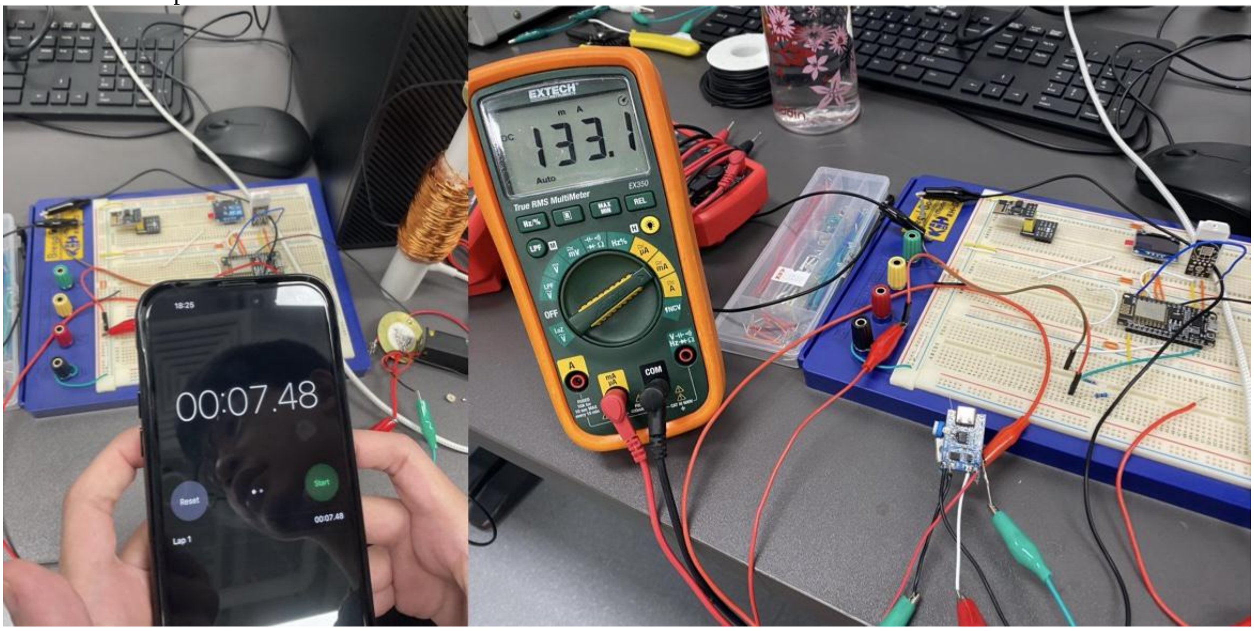

Figure 42: IoT Wi-Fi connection time current consumption per cycle

The NodeMCU took 7.48 second connect and transfer values via Wi-Fi. The MCU itself consume around 100mA but in this application there are also OLED screen and external sensors hence it consumes around 133.1mA per cycle. For an hour consumption,

$$Current\ consumption\ per\ cycle = 133.1mA \times 7s = 995.5mAs$$
$$Current\ sonsumption\ per\ hour = 6 \times 995.5mAs = 5973mAs$$
$$Therefore\ in\ mAh = 5973mAs \div 3600s = 1.65mAh$$

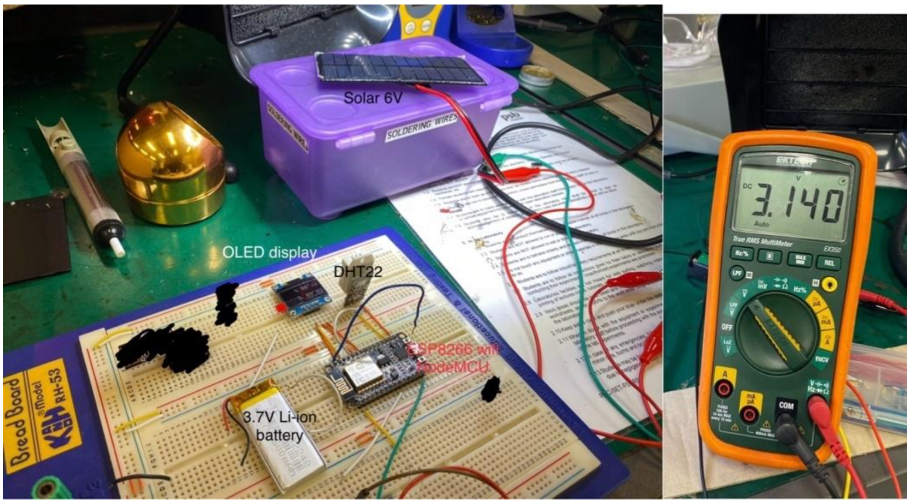

Figure 43: Indoor Solar Testing and voltage output

Figure 44: Outdoor Testing (Day mode) and battery voltage

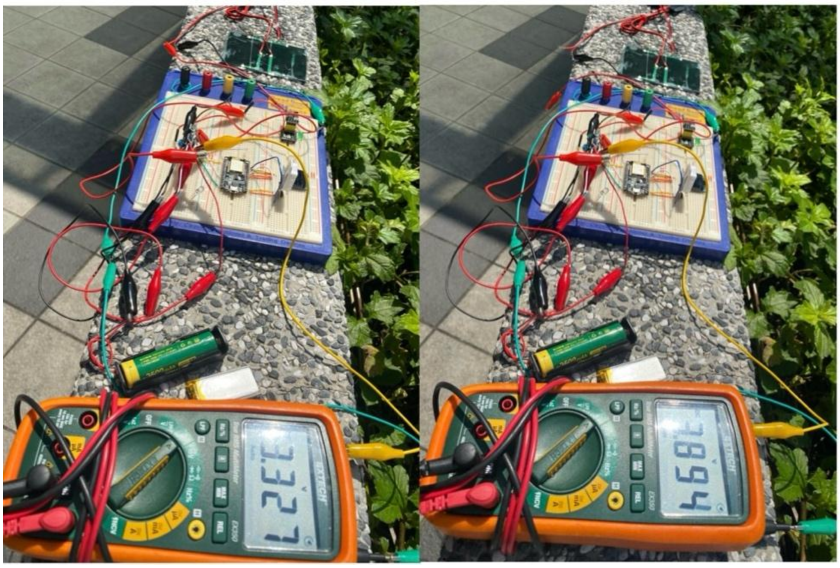

Figure 45: Outdoor Testing Night Mode (Drawing Battery Power)

Discussion

To simulate the bad weather or no sunlight condition, the solar is tested indoor and it can only provide 3.1V which can lead the MCU performance drop. Therefore, load sharing circuit is introduced and as from the results above the performance increase and it can charge and provide energy at the same time for IoT application. The circuit will automatically draw power from the battery when there is no sunlight or on cloudy days. The above results from Figure 56 also showing that the battery is charging.

Mobile battery monitoring layouts

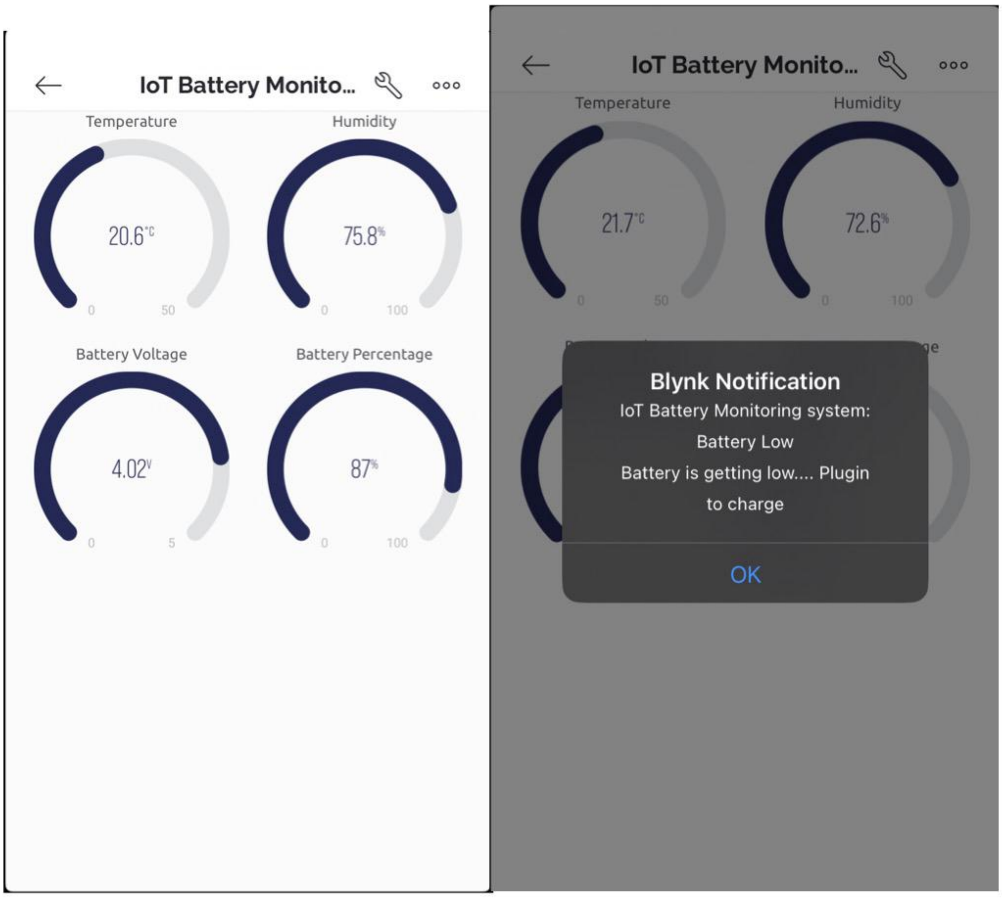

Figure 46: Blynk Mobile IoT Battery monitoring layout and Notifications result

If the battery is below 3 or 3V the Blynk cloud will send notification to the user to recharge the battery.

Thermal electric generator Practical Test results

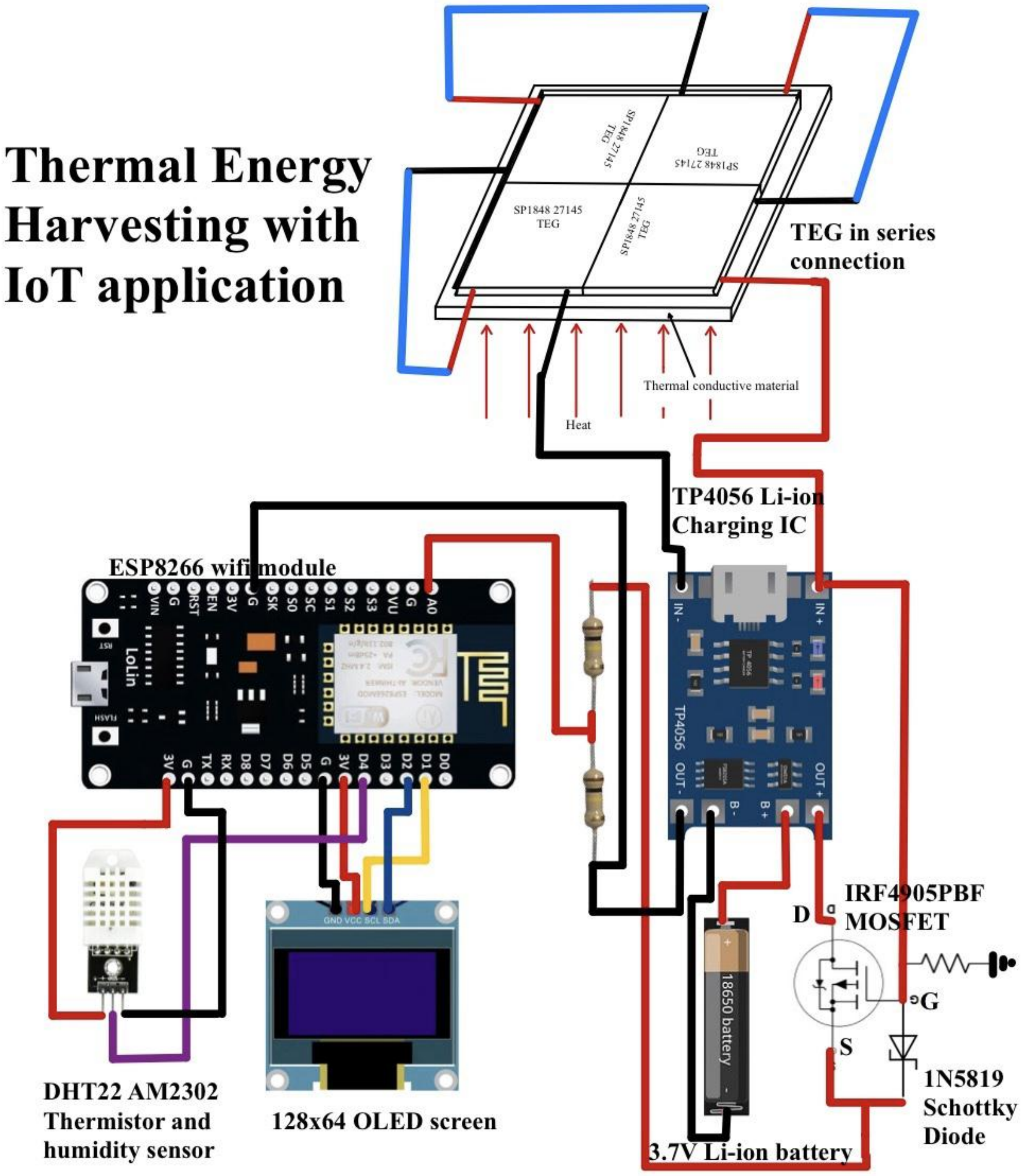

Figure 47: Thermal Electric generator with IoT

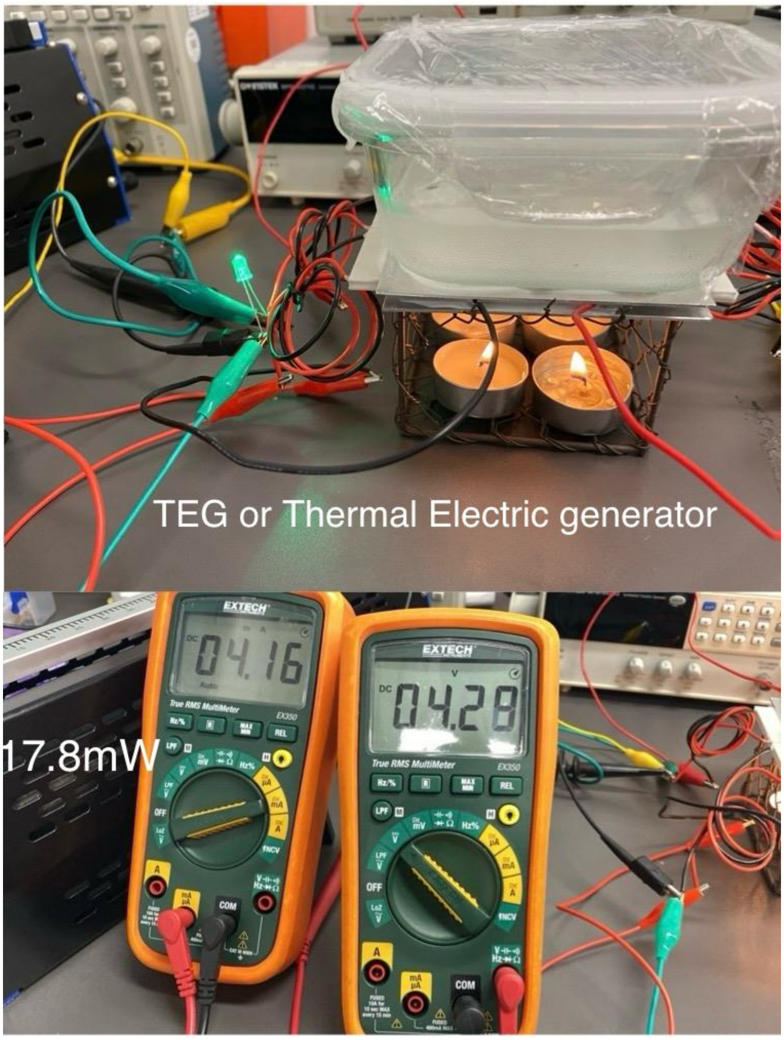

Figure 48: Thermal Electric generator

TEG or thermal electric generators are connected in series with various values of loads the Output power results are as shown in the below figure.

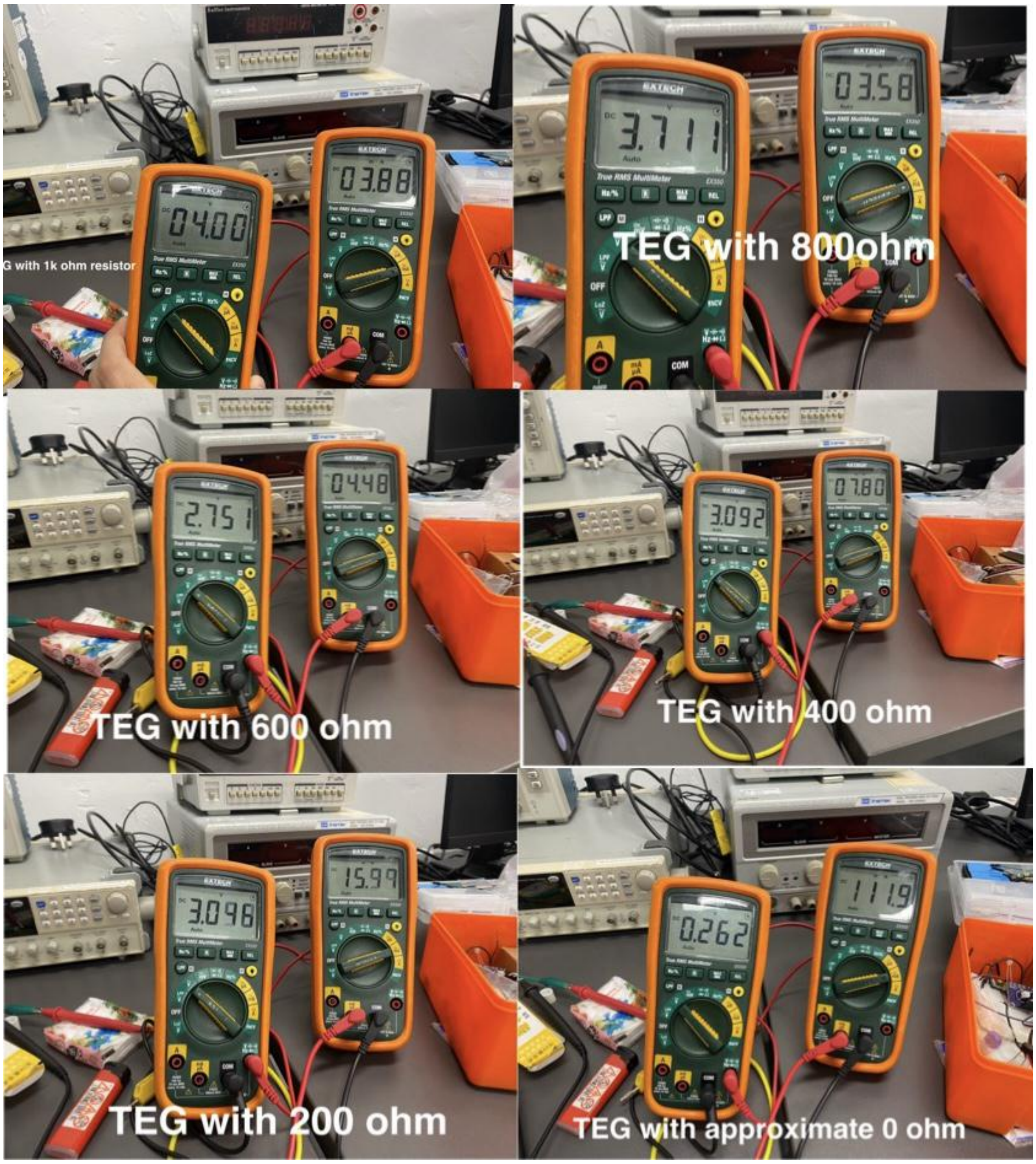

Figure 49: TEG power generation Results

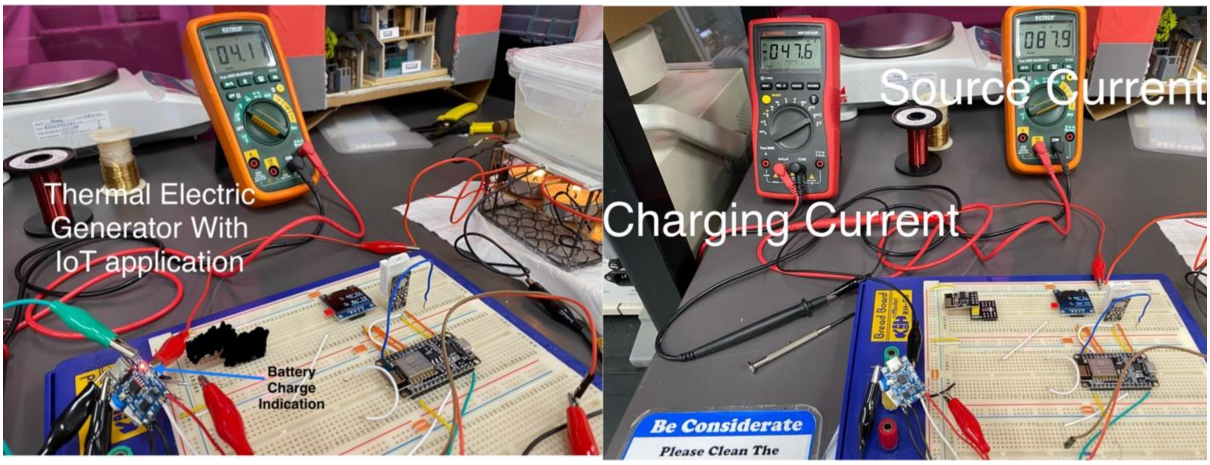

Figure 50: TEG with IoT application

Discussion

The TEG in this project is generate power with the ice bath water and heat from the Tea light candles. However in this design, the thermal conductivity between TEG and Ice bath water is poor due to the uneven surface of the container. Therefore the heat plaster or heat paste is applied to both the surface of the TEG and the glass surface. The material chosen for ice bath container is glass due to the longer usage of time since other materials such as iron, aluminium have high thermal conductivity point and can melt the ice very fast. The voltage and current produce will be higher but the ice has to add indefinitely. Hence the glass is used as the ice bath container. The Surface of the mini stove is rather small. We can improve the thermal conductivity and power generation by modifying the design of the mini stove.

Magnetic and Piezoelectric Generator Practical results

Circuit Diagram

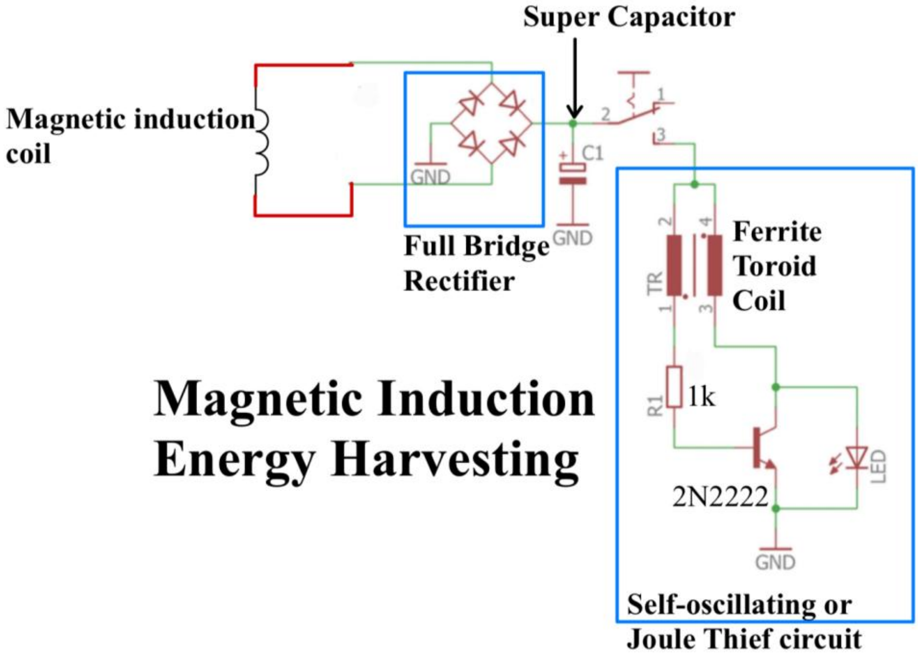

Figure 51: Overall Circuit Diagram of Motion generator

In this project the piezoelectric generator and magnetic generator will combined as a motion generator. If the motion generator cannot generate enough power the piezoelectric transducers will help the magnetic generator to generate more energy. According to the circuit diagram the sources are connected in series such that the voltage will be higher. Since all the sources are AC sources the bridge rectifier is required to store energy as the DC storage. As for the storage unit 1F supercapacitor is applied since super capacitors can store energy faster than the normal capacitors and it will act like a battery for the load. The energy harvested will be power for the LED and the whole generator will act like a battery less torch.

Design and Practical results

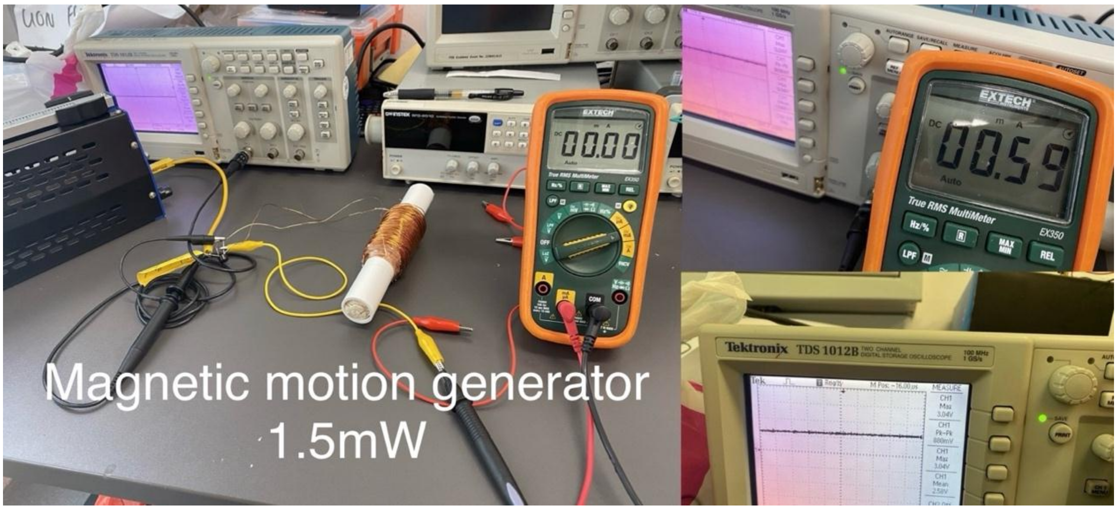

Figure 52: Magnetic Motion Generator Results

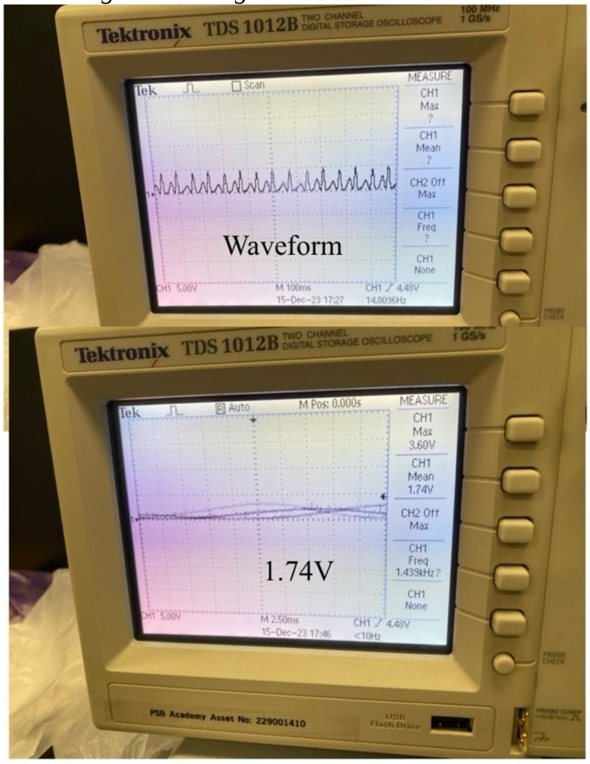

Figure 53: Waveform and voltage Before combining.

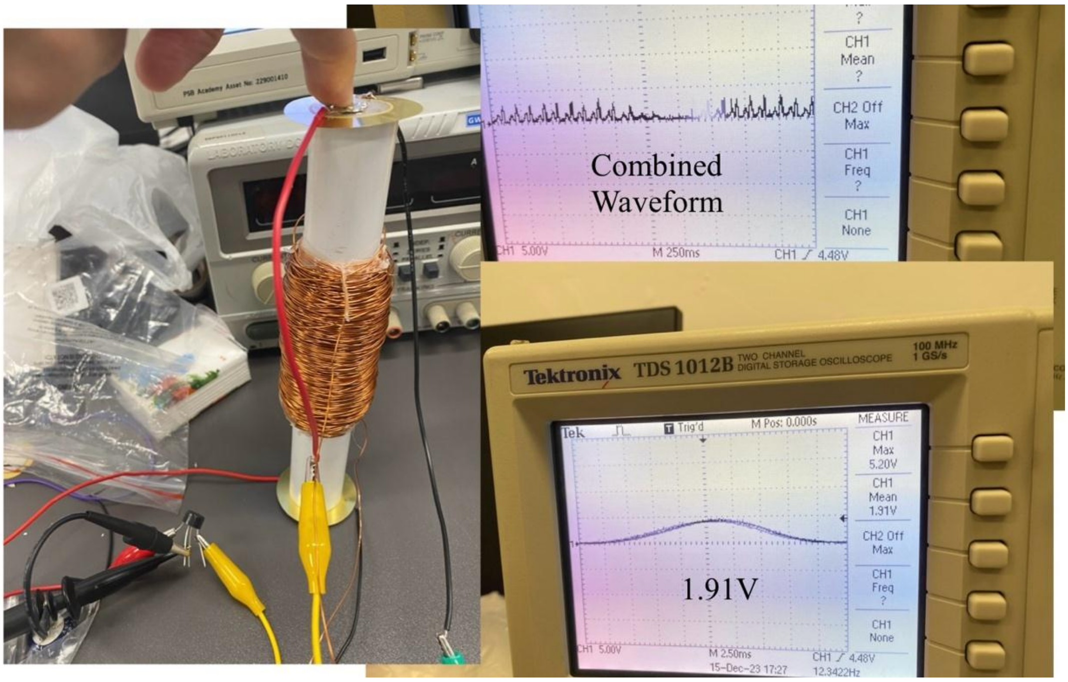

Figure 54: Prototype Design, waveform, and Voltage

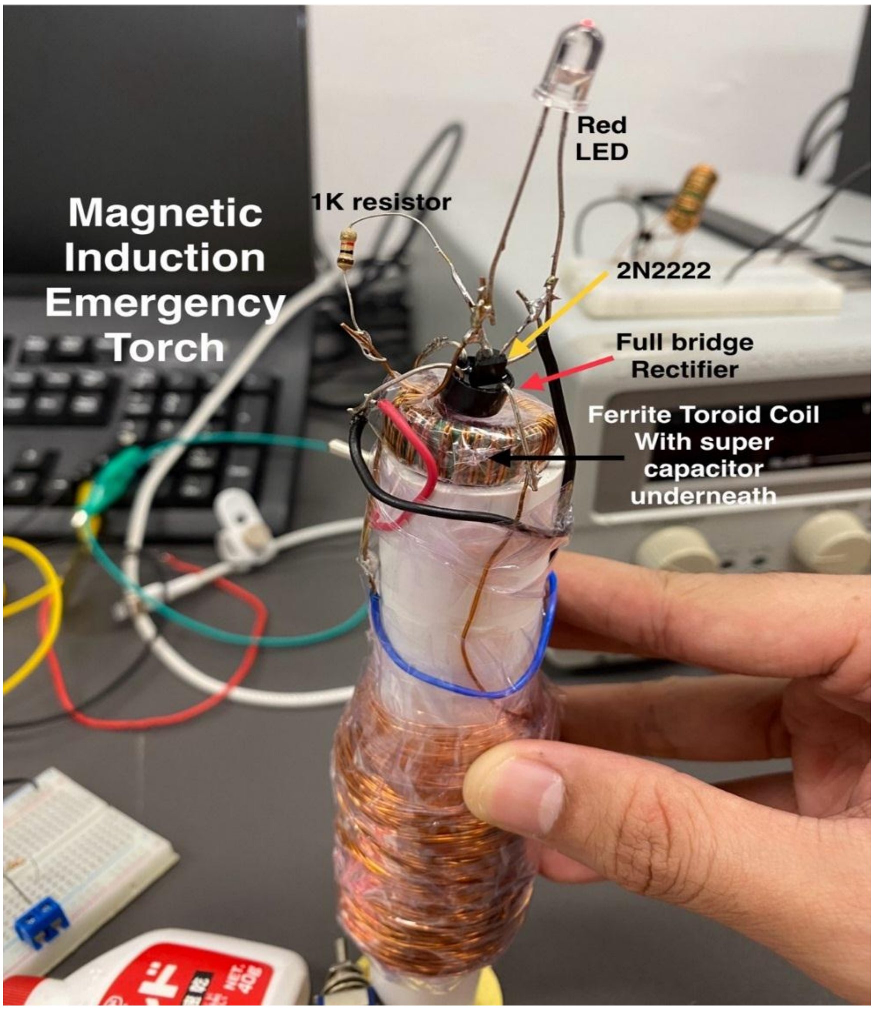

Figure 54: Prototype Design of shaking torch

Discussion

As expected, the Voltage is slightly higher compared to combined and uncombined prototype. The peak waveform is 3.6V form the magnetic generator alone after combing two sources, the peak voltage become 5.2V. Combined with Joule Thief circuit, this prototype can harvest energy from the motion and can power the LED acting like an Emergency Motion Torch.

VIII. CONCLUSION

Based on the results I got from the prototypes, Solar is the most powerful energy harvester among the other sources I choose. It can alone provide energy for the IoT device without any help of another sources. It can extend the lifetime of the battery while giving power to the IoT itself in the daytime. While the IoT draw power form the battery during nighttime or cloudy days.

The second most powerful Energy harvesting source is TEG. If the prototype has the better design and better thermal conductivity, this prototype can also help other sources to boost up Voltage. It can easily power the green LED as show in the Figure 59. With better thermal conduction, it can also power small IoT projects.

As for the motion generator it can generate just enough energy for the LED light. combined with piezo, it can harvest more and provide more energy to the supercapacitor. This prototype can also use as an emergency shaking torch in the place that the electricity can hard to harvest.

In this project the following scenario must meet for better performance of the prototypes for all of the sources.

Solar: The solar must use in outdoor for best efficiency. In door light can lead the IoT to disconnect with wi-fi and drop the performance of the MCU.

Thermal electric Generator: The ice needs to add constantly for greater temperature difference and thus more power can generate.

Magnetic induction Torch: Faster oscillation for better brightness of LED.

Table 5 illustrates the tasks that I have completed. As can be seen below, I have completed all of the functional requirements under the “Must Have” and “Should Have” category. Hence, the overall project objective that is set from the start has been met. On top of that, two of the tasks from “Should Have” are also done as an add-on improvement to the overall project.

Table 9: Power Harvested table from each source and its charging current to battery.

Sources	Voltage	Current (mA)	Charging Current(mA)	Power (mW)
Solar(indoor)	6.55(max)	6.36mA	-	-
Solar(outdoor)	4.02	136	123.8	546.72
Thermal	4.11	87.9	47.6	361.27
Magnetic	2.55	0.59	-	1.5

This energy harvesting systems successfully harvested energy from various sources and store energy for respective applications.

Solar harvested – 546.72mW with charging current of 123.8mA
Battery capacity -2500mAh
Estimated charging time = 2500mAh÷123.8mA= 20.19h

Thermal Electric generator harvested 361.27mW with charging current of 47.6mA
Estimated charging time = 2500mAh ÷47.6mA = 52h

Magnetic induction generator 1.5mW. With the future improvements it can even charge smarts phones.

Future Improvements

Solar: From the practical results above solar can power the IoT application while charging the battery. Using multiple panels can improve charging time.

Thermal Results: With better design & thermal conduction charge, with bigger temperature differential on certain weather conditions it can also generate like solar.

Magnetic: More winding of the induction can induce more current and voltage to have better efficiency.

REFERENCE

[1]. Munaz, A.; Lee, B.-C.; Chung, G.-S. A Study on Vibration-Driven Electromagnetic Energy Harvester with Multi-pole Magnets. Sens. Actuators A Phys. 2012, 201, 134–140.

[2]. Bhuyan, S. (2023, February 1). Electromagnetic induction: Definition, examples, & applications. Science Facts. Retrieved April 22, 2023, from https://www.sciencefacts.net/electromagnetic-induction.html

[3]. Yuen, S.C.L.; Lee, J.M.H.; Li, W.J.; Leong, P.H.W. An AA-Sized Vibration Based Microgenerator for Wireless Sensors. IEEE Pervasive Comput. 2007, 6, 65.

[4]. Jackson, S. L. (n.d.). Coreless brushed DC Motors. Automate. Retrieved April 22, 2023, from https://www.automate.org/products/moons-industries-inc/coreless-brushed-dc-motors

[5]. Peng, W.; Wei, L.; Lufeng, C. Design and fabrication of a micro electromagnetic vibration energy harvester. J. Semicond. 2011, 32, 104009.

[6]. Kok, C.L.; Ho, C.K.; Tanjodi, N.; Koh, Y.Y. A Novel Water Level Control System for Sustainable Aquarium Use. Electronics 2024, 13, 2033. doi: 10.3390/electronics13112033

[7]. Bernocchi, J. (n.d.). Coreless Motors. Servotecnica. Retrieved April 22, 2023, from https://www.servotecnica.com/en/resources/motion-blog-en/what-are-the-coreless-motors/

[8]. Mescia, L.; Losito, O.; Prudenzano, F. Innovative Materials and Systems for Energy Harvesting Applications; IGI Global: Hershey, PA, USA, 2015; pp. 254–259, 271–272.

[9]. Sudevalayam, S.; Kulkarni, P. Energy Harvesting Sensor Nodes: Survey and Implications. IEEE Commun. Surv. Tutor. 2011, 13, 443–461.

[10]. Hu, Y.T.; Xue, H.; Hu, H.P. Chapter 3 Piezoelectric Power/Energy Harvesters. In Analysis of Piezoelectric Structures and Devices; De Gruyter: Berlin, Germany, 2013; pp. 72–75.

[11]. Priya, S.; Song, H.; Zhou, Y.; Varghese, R.; Chopra, A.; Kim, S.; Kanno, I.; Wu, L.; Ha, D.S.; Ryu, J.; et al. A Review on Piezoelectric Energy Harvesting: Materials, Methods, and Circuits. Energy Harvest. Syst. 2017, 4, 3–39.

[12]. Kok, C.L.; Siek, L. Designing a Twin Frequency Control DC-DC Buck Converter Using Accurate Load Current Sensing Technique. Electronics 2024, 13, 45. doi: 10.3390/electronics13010045

[13]. Y. -W. Chong, W. Ismail, K. Ko and C. -Y. Lee, "Energy Harvesting For Wearable Devices: A Review," in IEEE Sensors Journal, vol. 19, no. 20, pp. 9047-9062, 15 Oct.15, 2019, doi: 10.1109/JSEN.2019.2925638

[14]. Halim, M.A.; Cho, H.; Salauddin, M.; Park, J.Y. A miniaturized electromagnetic vibration energy harvester using flux-guided magnet stacks for human-body-induced motion. Sens. Actuators A Phys. 2016, 249, 23–29.

[15]. L. Mateu, C. Codrea, L. Nestor, M. Pollak, and P. Spies, “Human body energy harvesting thermogenerator for sensing applications,” in Proc. Int. Conf. Sensor Technol. Appl., Oct. 2007, pp. 366–372.

[16]. Kok, C.L.; Ho, C.K.; Tan, F.K.; Koh, Y.Y. Machine Learning-Based Feature Extraction and Classification of EMG Signals for Intuitive Prosthetic Control. Appl. Sci. 2024, 14, 5784. doi: 10.3390/app14135784

[17]. V. Leonov, “Thermoelectric energy harvesting of human body heat for wearable sensors,” IEEE Sensors J., vol. 13, no. 6, pp. 2284–2291, Jun. 2013.

[18]. D. C. Hoang, Y. K. Tan, H. B. Chng, and S. K. Panda, “Thermal energy harvesting from human warmth for wireless body area network in medical healthcare system,” in Proc. Int. Conf. Power Electron. Drive Syst. (PEDS), Nov. 2009, pp. 1277–1282.

[19]. S. Kim et al., “Ambient RF energy-harvesting technologies for self- sustainable standalone wireless sensor platforms,” Proc. IEEE, vol. 102, no. 11, pp. 1649–1666, Nov. 2014.

[20]. Tos, D. H. and H., & Instructables. (2017, October 11). Joule thief low Voltage Battery Charger. Instructables. https://www.instructables.com/Joule-Thief-Low-Voltage-Battery-Charger

[21]. Krikidis, S. Timotheou, S. Nikolaou, G. Zheng, D. W. K. Ng, and R. Schober, “Simultaneous wireless information and power transfer in modern communication systems,” IEEE Commun. Mag., vol. 52, no. 11, pp. 104–110, Nov. 2014.

[22]. Kok, C.L.; Fu, X.; Koh, Y.Y.; Teo, T.H. A Novel Portable Solar Powered Wireless Charging Device. Electronics 2024, 13, 403. doi: 10.3390/electronics13020403

[23]. Han, A. D. (2021, July 1). Neodymium magnets (NdFeB). Arnold Magnetic Technologies. Retrieved April 22, 2023, from https://www.arnoldmagnetics.com/products/neodymium-iron-boron-magnets/

[24]. J. A. G. Akkermans, M. C. van Beurden, G. J. N. Doodeman, and H. J. Visser, “Analytical models for low-power rectenna design,” IEEE Antennas Wireless Propag. Lett., vol. 4, pp. 187–190, 2005.

[25]. J. A. G. Akkermans, M. C. van Beurden, G. J. N. Doodeman, and H. J. Visser, “Analytical models for low-power rectenna design,” IEEE Antennas Wireless Propag. Lett., vol. 4, pp. 187–190, 2005.

[26]. C. R. Valenta and G. D. Durgin, “Harvesting wireless power: Survey of energy-harvester conversion efficiency in far-field, wireless power transfer systems,” IEEE Microw. Mag., vol. 15, no. 4, pp. 108–120, Jun. 2014.

[27]. D. Zhu, J. Wang, L. Siek, C. L. Kok, L. Qiu and Y. Zheng, "High accuracy time-mode duty-cycle-modulation-based temperature sensor for energy efficient system applications," 2014 International Symposium on Integrated Circuits (ISIC), Singapore, 2014, pp. 400-403, doi: 10.1109/ISICIR.2014.7029502.

[28]. D. Zhu, J. Wang, C. L. Kok, L. Siek and Y. Zheng, "A new time-mode on-chip oscillator-based low power temperature sensor," 2015 IEEE International Conference on Electron Devices and Solid-State Circuits (EDSSC), Singapore, 2015, pp. 411-414, doi: 10.1109/EDSSC.2015.7285138.

[29]. S. Mandal, L. Turicchia, and R. Sarpeshkar, “A low-power, battery-free tag for body sensor networks,” IEEE Pervasive Comput., vol. 9, no. 1, pp. 71–77, Mar. 2010.

[30]. X. Zhang, H. Jiang, L. Zhang, C. Zhang, Z. Wang, and X. Chen, “An energy-efficient ASIC for wireless body sensor networks in medical applications,” IEEE Trans. Biomed. Circuits Syst., vol. 4, no. 1, pp. 11–18, Feb. 2010.

[31]. Kok, C.L.; Dai, Y.; Lee, T.K.; Koh, Y.Y.; Teo, T.H.; Chai, J.P. A Novel Low-Cost Capacitance Sensor Solution for Real-Time Bubble Monitoring in Medical Infusion Devices. Electronics 2024, 13, 1111. doi: 10.3390/electronics13061111

[32]. L. Xia, J. Cheng, N. E. Glover, and P. Chiang, "0.56 V, –20 dBm RF-powered, multi-node wireless body area network system-on-a-chip with harvesting-efficiency tracking loop," IEEE J. Solid-State Circuits, vol. 49, no. 6, pp. 1345–1355, Jun. 2014.

[33]. P. Jokic and M. Magno, "Powering smart wearable systems with flexible solar energy harvesting," 2017 IEEE International Symposium on Circuits and Systems (ISCAS), Baltimore, MD, USA, 2017, pp. 1-4, doi: 10.1109/ISCAS.2017.8050615.

[34]. Kok, C.L.; Ho, C.K.; Dai, Y.; Lee, T.K.; Koh, Y.Y.; Chai, J.P. A Novel and Self-Calibrating Weighing Sensor with Intelligent Peristaltic Pump Control for Real-Time Closed-Loop Infusion Monitoring in IoT-Enabled Sustainable Medical Devices. Electronics 2024, 13, 1724. doi: 10.3390/electronics13091724

[35]. G. V. Merrett, H. Huang, and N. M. White, "Modeling the effect of orientation on human-powered inertial energy harvesters," IEEE Sensors J., vol. 15, no. 1, pp. 434–441, Jan. 2015.

[36]. W. D. McArdle, F. I. Katch, and V. L. Katch, "Exercise physiology: Energy, nutrition, and human performance," 5th ed. New York, NY, USA: Williams & Wilkins, 2001.

[37]. F. Akhtar and M. H. Rehmani, "Energy harvesting for self-sustainable wireless body area networks," IT Prof., vol. 19, no. 2, pp. 32–40, Mar./Apr. 2017.

[38]. Yang, Dr. D. (2018, October 17). Recent advances in flexible perovskite solar ... - wiley online library. Flexible Solar to fabric Applications. https://onlinelibrary.wiley.com/doi/10.1002/anie.201809781

[39]. H. C. Van Nguyen, "Implantable, miniaturized microbial fuel cell," Univ. California Berkeley, Berkeley, CA, USA, Tech. Rep. UCB/EECS- 2012-249, 2012.

[40]. W. Jia, G. Valdés-Ramírez, A. J. Bandodkar, J. R. Windmiller, and J. Wang, "Epidermal biofuel cells: Energy harvesting from human perspiration," Angew. Chem. Int. Ed., vol. 52, no. 28, pp. 7233–7236, 2013.

[41]. J. Mendoza and A. Sánchez, "On the Design of a RF Schottky Diode Rectifier for Energy Harvesting Applications," 2018 IEEE International Autumn Meeting on Power, Electronics and Computing (ROPEC), Ixtapa, Mexico, 2018, pp. 1-6, doi: 10.1109/ROPEC.2018.8661448.

[42]. M. Nesarajah and G. Frey, "Thermoelectric power generation: Peltier element versus thermoelectric generator," IECON 2016 - 42nd Annual Conference of the IEEE Industrial Electronics Society, Florence, Italy, 2016, pp. 4252-4257, doi: 10.1109/IECON.2016.7793029.

[43]. H. -P. Wong and Z. Dahari, "Human body parts heat energy harvesting using thermoelectric module," 2015 IEEE Conference on Energy Conversion (CENCON), Johor Bahru, Malaysia, 2015, pp. 211-214, doi: 10.1109/CENCON.2015.7409541.

[44]. Katylin, A. A. (n.d.). Dimensions of average male human being. Retrieved April 22, 2023, from https://www.researchgate.net/figure/Dimensions-of-average-male-human-being-23_fig1_283532449

[45]. P. Luo, D. Peng, Y. Wang and X. Zheng, "Review of Solar Energy Harvesting for IoT Applications," 2018 IEEE Asia Pacific Conference on Circuits and Systems (APCCAS), Chengdu, China, 2018, pp. 512-515, doi: 10.1109/APCCAS.2018.8605651.

[46]. Kok, C.L.; Chia, K.J.; Siek, L. A 87 dB SNR and THD+N 0.03% HiFi Grade Audio Preamplifier. Electronics 2024, 13, 118. doi: 10.3390/electronics13010118

[47]. Aung, K.H.H.; Kok, C.L.; Koh, Y.Y.; Teo, T.H. An Embedded Machine Learning Fault Detection System for Electric Fan Drive. Electronics 2024, 13, 493. doi: 10.3390/electronics13030493

[48]. Chen, J.; Teo, T.H.; Kok, C.L.; Koh, Y.Y. A Novel Single-Word Speech Recognition on Embedded Systems Using a Convolution Neuron Network with Improved Out-of-Distribution Detection. Electronics 2024, 13, 530. doi: 10.3390/electronics13030530

[49]. Don Chua, W.F.; Lim, C.L.; Koh, Y.Y.; Kok, C.L. A Novel IoT Photovoltaic-Powered Water Irrigation Control and Monitoring System for Sustainable City Farming. Electronics 2024, 13, 676. doi: 10.3390/electronics13040676

[50]. Kok, C.L.; Kusuma, I.M.B.P.; Koh, Y.Y.; Tang, H.; Lim, A.B. Smart Aquaponics: An Automated Water Quality Management System for Sustainable Urban Agriculture. Electronics 2024, 13, 820. doi: 10.3390/electronics13050820

[51]. X. Lu, P. Wang, D. Niyato, D.I. Kim, and Z. Han, "Wireless Charging Technologies: Fundamentals, Standards, and Network Applications," IEEE Communications Surveys & Tutorials, vol. 18, no. 2, pp. 1413-1452, Secondquarter 2016. doi: 10.1109/COMST.2016.2519478

[52]. Kok, C.L.; Tang, H.; Teo, T.H.; Koh, Y.Y. A DC-DC Converter with Switched-Capacitor Delay Deadtime Controller and Enhanced Unbalanced-Input Pair Zero-Current Detector to Boost Power Efficiency. Electronics 2024, 13, 1237. doi: 10.3390/electronics13071237

[53]. T. Zhang, Z. Chen, S. Yang, and K.S. Kwak, "Energy-Efficient Data Collection with Self-Powered IoT Devices: A Circuit-Information-Processing Co-Design," IEEE Internet of Things Journal, vol. 6, no. 5, pp. 8362-8371, Oct. 2019. doi: 10.1109/JIOT.2019.2908051

[54]. Kok, C.L.; Tan, T.C.; Koh, Y.Y.; Lee, T.K.; Chai, J.P. Design and Testing of an Intramedullary Nail Implant Enhanced with Active Feedback and Wireless Connectivity for Precise Limb Lengthening. Electronics 2024, 13, 1519. doi: 10.3390/electronics13081519

[55]. Koh, Y.Y.; Kok, C.L.; Ibraahim, N.; Lim, C.G. Smart Water ATM with Arduino Integration, RFID Authentication, and Dynamic Dispensing for Enhanced Hydration Practices. Electronics 2024, 13, 1657. doi: 10.3390/electronics13091657

[56]. M. Magno and L. Benini, "An Ultra-Low Power High Sensitivity Wake-Up Radio Receiver With Addressing Capability," IEEE Transactions on Circuits and Systems I: Regular Papers, vol. 64, no. 2, pp. 411-420, Feb. 2017. doi: 10.1109/TCSI.2016.2615199

[57]. A. Dolara, G. C. Lazaroiu, and S. Leva, "Energy-Efficient Cloud IoT System Exploiting Renewable Energy," IEEE Transactions on Industrial Informatics, vol. 16, no. 4, pp. 2643-2651, April 2020. doi: 10.1109/TII.2019.2939344

[58]. P. Hu, M. Qiu, and E.H.-M. Sha, "Energy-Aware Scheduling for Real-Time Multiprocessor Systems with Uncertain Task Execution Time," IEEE Transactions on Computers, vol. 66, no. 7, pp. 1137-1148, July 2017. doi: 10.1109/TC.2017.2685620

[59]. Kok, C.L.; Ho, C.K.; Lee, T.K.; Loo, Z.Y.; Koh, Y.Y.; Chai, J.P. A Novel and Low-Cost Cloud-Enabled IoT Integration for Sustainable Remote Intravenous Therapy Management. Electronics 2024, 13, 1801. doi: 10.3390/electronics13101801

[60]. Teo, B.C.T.; Lim, W.C.; Venkadasamy, N.; Lim, X.Y.; Kok, C.L.; Siek, L. A CMOS Rectifier with a Wide Dynamic Range Using Switchable Self-Bias Polarity for a Radio Frequency Harvester. Electronics 2024, 13, 1953. doi: 10.3390/electronics13101953

[61]. Kok, C.L.; Ho, C.K.; Teo, T.H.; Kato, K.; Koh, Y.Y. A Novel Implementation of a Social Robot for Sustainable Human Engagement in Homecare Services for Ageing Populations. Sensors 2024, 24, 4466. doi: 10.3390/s24144466

[62]. P. Mitcheson, E. Yeatman, G. Rao, A. Holmes, and T. Green, "Energy Harvesting From Human and Machine Motion for Wireless Electronic Devices," Proceedings of the IEEE, vol. 96, no. 9, pp. 1457-1486, Sept. 2008. doi: 10.1109/JPROC.2008.927494

[63]. R. H. Myers, M. V. Scanlon, and B. M. Kwasa, "Adaptive Energy Harvesting Systems for Self-Sustained Wireless Sensors," IEEE Sensors Journal, vol. 15, no. 12, pp. 7355-7363, Dec. 2015. doi: 10.1109/JSEN.2015.2488788

[64]. J. L. Chao, K. Chang, and R. B. Zadeh, "Analysis of Energy Harvesting Communications With Battery Inertial Effects," IEEE Transactions on Wireless Communications, vol. 18, no. 2, pp. 957-968, Feb. 2019. doi: 10.1109/TWC.2018.2888704

[65]. C. -L. Kok, Q. Huang, D. Zhu, L. Siek and W. M. Lim, "A fully digital green LDO regulator dedicated for biomedical implant using a power-aware binary switching technique," 2012 IEEE Asia Pacific Conference on Circuits and Systems, Kaohsiung, Taiwan, 2012, pp. 5-8, doi: 10.1109/APCCAS.2012.6418957.

[66]. X. Zhang, J. Wang, and Y. Zhao, "Wireless Information and Power Transfer in Cooperative Relay Networks With Opportunistic Scheduling," IEEE Transactions on Vehicular Technology, vol. 67, no. 3, pp. 2383-2397, March 2018. doi: 10.1109/TVT.2017.2776291

[67]. S. R. Anton and D. J. Inman, "Vibration Energy Harvesting for Unmanned Aerial Vehicles," IEEE Transactions on Power Electronics, vol. 26, no. 1, pp. 283-290, Jan. 2011. doi: 10.1109/TPEL.2010.2051770

[68]. H. Yang, S. Xiong, P. Chen, and Y. Zhang, "Thermoelectric Energy Harvesting for Self-Powered Sensors in Smart Homes," IEEE Transactions on Industrial Electronics, vol. 63, no. 6, pp. 3722-3732, June 2016. doi: 10.1109/TIE.2016.2521160

[69]. C. -L. Kok, X. Li, L. Siek, D. Zhu and J. J. Kong, "A switched capacitor deadtime controller for DC-DC buck converter," 2015 IEEE International Symposium on Circuits and Systems (ISCAS), Lisbon, Portugal, 2015, pp. 217-220, doi: 10.1109/ISCAS.2015.7168609.

[70]. M. Seyedi, B. Kibret, D.T.H. Lai, and M. Faulkner, "A Survey on Intrabody Communications for Body Area Network Applications," IEEE Transactions on Biomedical Engineering, vol. 60, no. 8, pp. 2067-2079, Aug. 2013. doi: 10.1109/TBME.2013.2254714

[71]. C. Tachtatzis, W. H. Chin, M. McCann, and S. McLaughlin, "A Survey on Wireless Body Area Networks for E-Health," IEEE Communications Surveys & Tutorials, vol. 16, no. 2, pp. 1658-1686, Secondquarter 2014. doi: 10.1109/SURV.2014.031914.00092

[72]. T. Rakia, H. Ghazzai, A. Kadri, and M.S. Alouini, "Energy Efficiency in Internet of Things: A System-Level Approach," IEEE Transactions on Green Communications and Networking, vol. 3, no. 2, pp. 461-473, June 2019. doi: 10.1109/TGCN.2019.2909305

[73]. C. L. Kok, T. H. Teo, Y. Y. Koh, Y. Dai, B. K. Ang and J. P. Chai, "Development and Evaluation of an IoT-Driven Auto-Infusion System with Advanced Monitoring and Alarm Functionalities," 2024 IEEE International Symposium on Circuits and Systems (ISCAS), Singapore, Singapore, 2024, pp. 1-5, doi: 10.1109/ISCAS58744.2024.10558602.

[74]. M. Z. A. Bhuiyan, J. Wu, and G. Wang, "eSDF: A Framework for Efficient Solar Data Forwarding in Wireless Sensor Networks With Ambient Energy Harvesting," IEEE Transactions on Computers, vol. 66, no. 7, pp. 1231-1243, July 2017. doi: 10.1109/TC.2017.2666798

[75]. J. Qin, H. Zhang, Z. Xu, and D. Li, "Joint Power and Energy Harvesting Time Allocation in Full-Duplex SWIPT IoT Networks," IEEE Transactions on Green Communications and Networking, vol. 3, no. 3, pp. 636-647, Sept. 2019. doi: 10.1109/TGCN.2019.2926712

[76]. C. -L. Kok, L. Siek and W. M. Lim, "An ultra-fast 65nm capacitorless LDO regulator dedicated for sensory detection using a direct feedback dual self-reacting loop technique," 2012 IEEE International Symposium on Radio-Frequency Integration Technology (RFIT), Singapore, 2012, pp. 31-33, doi: 10.1109/RFIT.2012.6401604.

[77]. C. Wu et al., "Asymmetrical Dead-Time Control Driver for Buck Regulator," in IEEE Transactions on Very Large Scale Integration (VLSI) Systems, vol. 24, no. 12, pp. 3543-3547, Dec. 2016, doi: 10.1109/TVLSI.2016.2551321.

[78]. G. Pan and J. M. Rabaey, "Design of Ultra-Low Power Universal Asynchronous Receivers and Transmitters for Wireless Body Area Networks," IEEE Transactions on Circuits and Systems I: Regular Papers, vol. 63, no. 4, pp. 496-506, April 2016. doi: 10.1109/TCSI.2016.2537318

[79]. C. -L. Kok and L. Siek, "A novel 2-terminal zener voltage reference," 2011 IEEE 54th International Midwest Symposium on Circuits and Systems (MWSCAS), Seoul, Korea (South), 2011, pp. 1-4, doi: 10.1109/MWSCAS.2011.6026364.